Open-File Report 96-4
Field Trip No. 11

The Slumgullion Landslide Hinsdale County Colorado

By
Robert W. Fleming, Rex L. Baum,
and William Z. Savage
U. S. Geological Survey
Box 25046, M.S. 966
Denver, CO 80225-0046

Colorado Geological Survey
Department of Natural Resources
Denver, Colorado
1996

THE SLUMGULLION LANDSLIDE, HINSDALE COUNTY, COLORADO

by Robert W. Fleming, Rex L. Baum, and William Z. Savage
U.S. Geological Survey
Box 25046, M.S. 966
Denver, CO 80225-0046

TOC

INTRODUCTION

This field trip to examine the kinematics of the Slumgullion landslide (Fig. 1) provides an opportunity to examine structural features produced by the movement of the landslide. Part of the landslide has been observed to be actively moving for at least the past 100 years, and features on the landslide surface are continuously created and destroyed by the movement.

The structural features that we can observe are along the active margins and within the body of the active landslide. Faults and fault zones are typical features along the active margins. The landslide flanks are characterized by strike-slip faults. Normal faults are typical of the uppermost parts of the landslide, and thrust faults are typical of the distal parts of the landslide. Within the body of the active landslide, structural features are produced by a change in the boundary geometry or by variations in the velocity of movement. The resulting deformation is characterized by stretching, shortening, and shearing.

Virtually every landslide contains deformational features that are a product of sliding. In the upslope parts, where active landslide material pulls away from nonmoving ground, the characteristic features are produced by stretching. At the downslope terminus, where the landslide toe is resisting movement, the characteristic features are produced by shortening. The amount of displacement varies over the landslide surface; from top to bottom, displacement goes from zero through a maximum value to zero again at the toe. The displacement differences produce internal deformation that appears as fractures at some places and as indirect indicators, such as stretched or buckled tree roots, in others.

By virtue of its great size, the Slumgullion landslide contains many different examples of deformational responses to continuous movement. The understanding of a large structural feature within the landslide begins with the observation of tiny fractures that serve as guides to deformation. The guide fractures can be interpreted in the context of expectable deformation in different parts of the landslide. Aggregates of guide features allow the interpretation of structures.

During this field trip we will make a traverse down the active landslide to observe these various guide features and show how information from them is used in the interpreta-

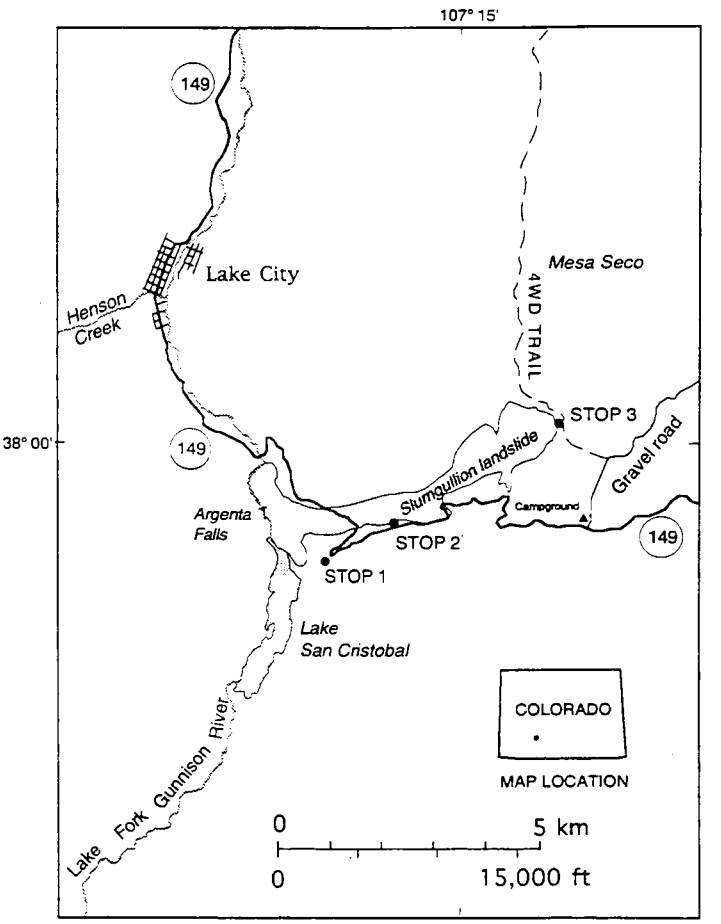

Figure 1. Map showing field trip route and stops. Trip departs from Lake City, Colorado, and follows Colorado State Highway 149 to the campground. From the campground, the trip heads north along the gravel road to the 4WD trail, and then up the trail to the head of the Slumgullion landslide. Participants walk down the landslide to waiting vehicle(s) parked near where Highway 149 crosses the south edge of the landslide.

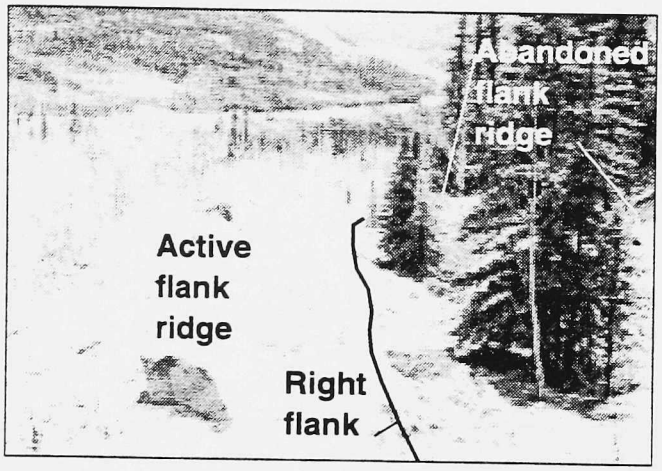

Figure 2. View of flank ridge at downslope end of pull-apart basin on right flank, looking southwest.

tion of structures. We will also see some structures, notably clay intrusions and extrusions and flank ridges, that are still poorly understood. In this traverse, we will see places where clay has been intruded along shear zones and places within the body of the landslide where it has extruded onto the ground surface. Perhaps the most striking features of the Slumgullion landslide are its flank ridges (Figs. 2 and 3). These are long ridges that form on both flanks and adjacent to strike-slip faults within the landslide. We have data on formation of the ridges (Fleming and Johnson, 1989; Baum and others, 1993), but lack coherent explanations of the processes of formation.

BACKGROUND

This field trip begins at Lake City, Colorado, and follows southbound Colorado Highway 149 (Fig. 1). Brief stops at two points provide an overview of most of the Slumgullion landslide. The trip continues along Highway 149 to Slumgullion Campground and then follows U.S. Forest Service roads to the head of the landslide. Participants hike down the slide from the head, making several stops to view landslide features, and return to waiting vehicles parked between the active toe and Highway 149.

The Slumgullion landslide (Figs. 4*A* and 4*B*) has been described by numerous investigators (Endlich, 1876; Howe, 1909; Atwood and Mather, 1932; Burbank, 1947; Crandell and Varnes, 1960, 1961; Keefer and Johnson, 1983; Varnes and Savage, 1996). The name Slumgullion, already ascribed to the landslide by miners at the time of Endlich's (1876) description, is an old term referring to a meat stew containing many different ingredients of various colors and having a variegated appearance. The earliest published photographs of the landslide were by Whitman Cross (pl. XXB in Howe, 1909). Crandell and Varnes (1961) first investigated the rates and history of movement.

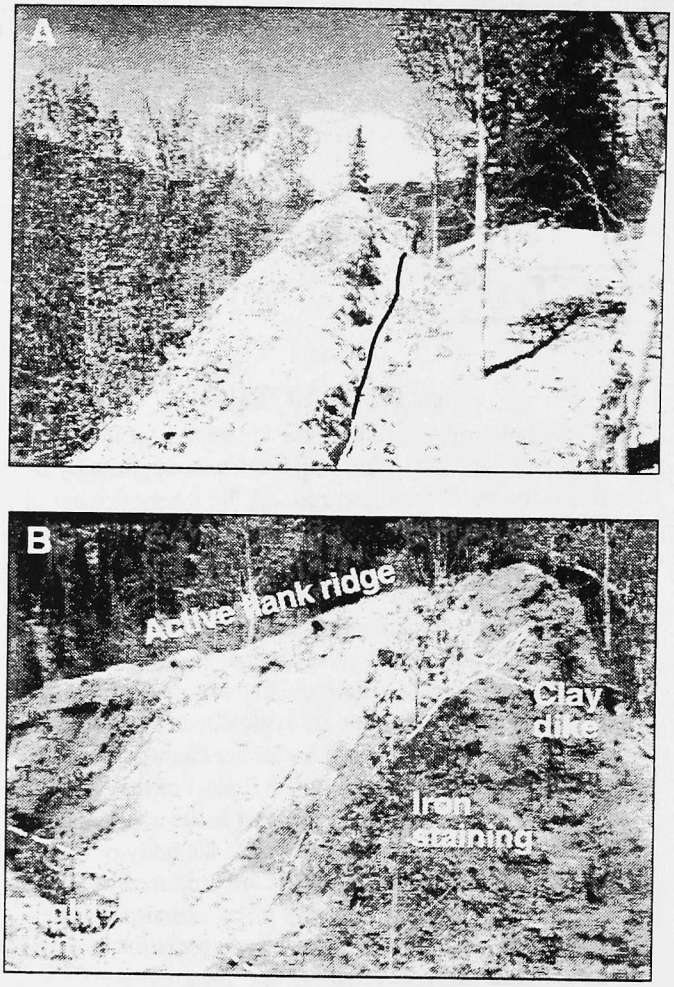

Figure 3. Views of an active flank ridge. *A*. Uphill end, looking southwest along right flank. Trees to left of ridge have deformed trunks. *B*. Downhill end looking east (Baum and Fleming, 1996). Exposed shear surface and clay dike inside right flank. A scarp at the outboard side of ridge (light area at center) exposes an emergent part of the lateral shear surface. This shear surface is between the crest and the trace of the right-lateral shear zone (shown by a dashed line). The scarp tapers from a height of about 2 m in foreground to 0 m in the background (about 20 m upslope, beyond left edge of photograph). The taper is consistent with screw-like movement along this part of the flank; the ridge growth is about 0.1 meter per meter of downslope of displacement. Annual movement here is about 3.5 m. The scarp is convex and is covered with sheared, highly plastic, blue-gray clay (liquid limit = 105, plasticity index = 77) that differs in color and texture from the stony, light-brown landslide material in the ridge. Movement at the shear zone has brought a tabular dike of blue-gray clay to the surface and injected the clay into the landslide materials.

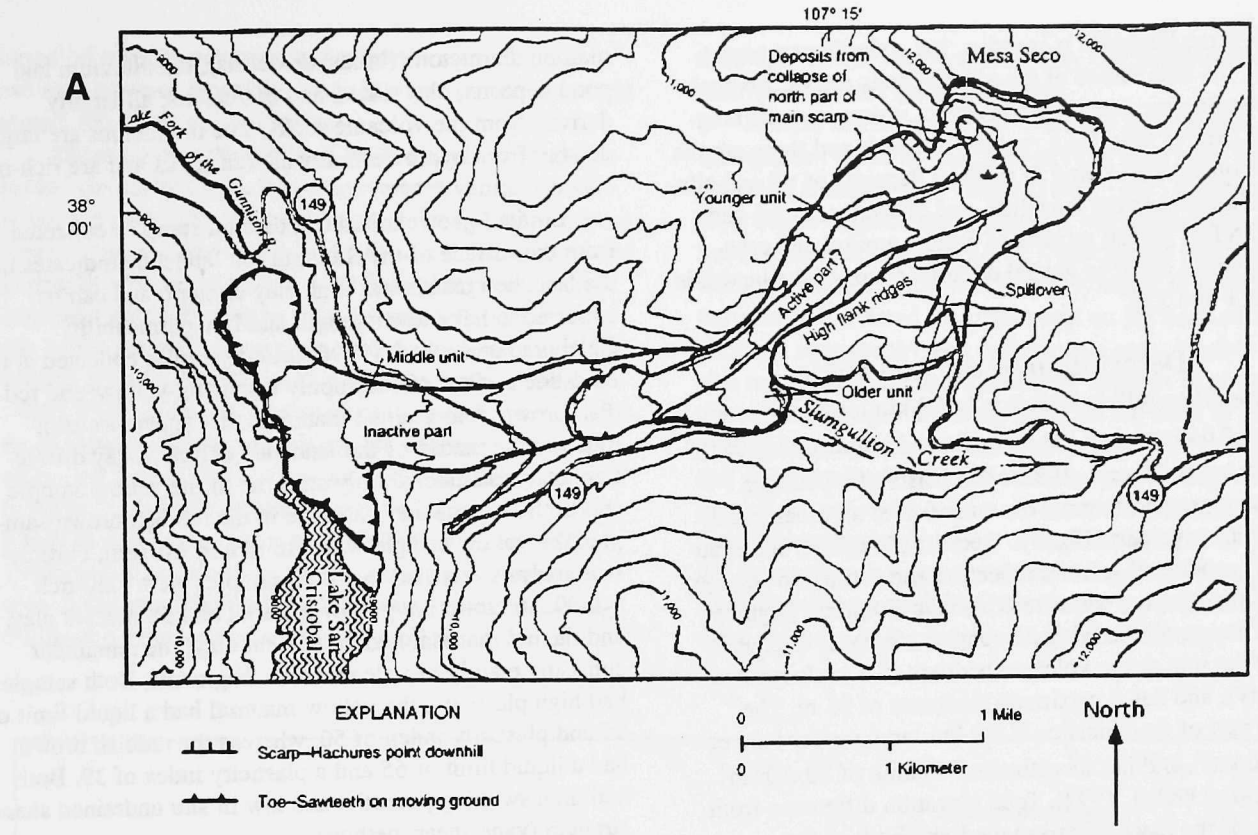

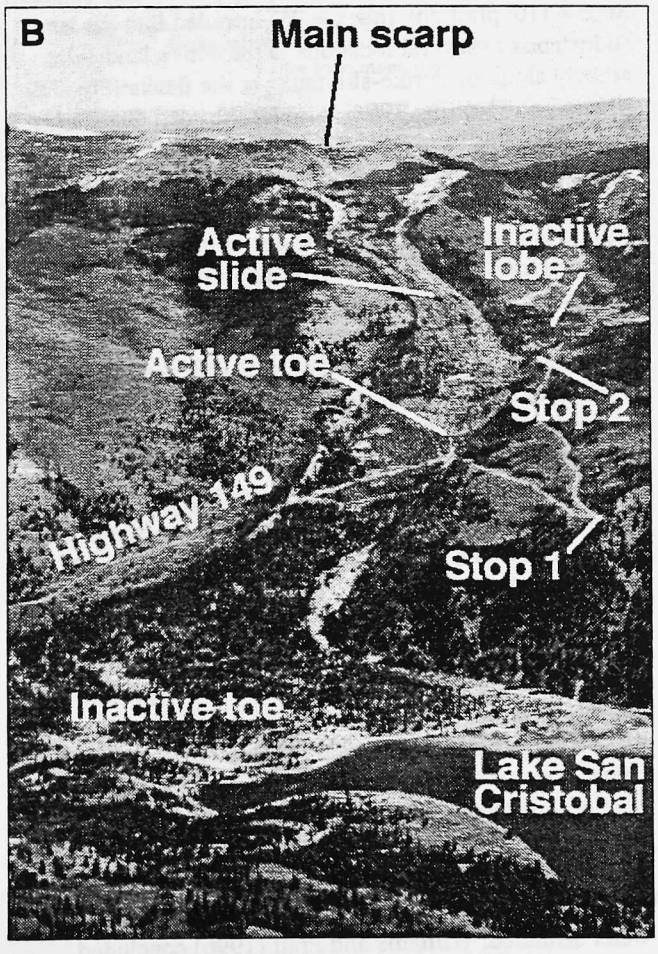

Figure 4. ***A.*** **Outline map of inactive and active parts of the Slumgullion landslide. The inactive part of the landslide is comprised of materials emplaced during at least two episodes of movement. The oldest known deposit (older unit) blocked Slumgullion Creek and spilled over a topographic divide farther upslope. The second oldest deposit (middle unit) blocked the Lake Fork of the Gunnison River, creating Lake San Cristobal. A collapse of the north side of the main scarp that provided a surcharge load to the upper part of the older landslide deposits may have triggered the currently active episode (younger unit).** ***B.*** **Aerial view of Slumgullion landslide, looking east (photograph by David J. Varnes, U.S. Geological Survey).**

In 1990, the U.S. Geological Survey (USGS), with the assistance of scientists provided by a cooperative agreement between the USGS and the Istituto di Ricerca per la Protezione Idrogeologica (IRPI) of the Italian National Research Council, began a new study of the Slumgullion earth flow (Varnes and Savage, 1996).

Geologic Setting

The Slumgullion landslide is located in the San Juan Mountains, a large early-Tertiary volcanic center in southwest Colorado (Fig. 1). The landslide formed as a result of collapse of hydrothermally altered volcanic materials in the rim of the Lake City Caldera (Lipman, 1976) on the south end of Mesa Seco (Fig. 4). The collapsed materials slid and flowed more than 6 km downhill to block the Lake Fork of the Gunnison River, creating Lake San Cristobal.

Most of the landslide is inactive, but a significant part within the boundaries of the older slide is active. Bedrock surrounding the landslide consists of volcanic rocks ranging in composition from rhyolite to basalt and these are the main constituents found in surficial deposits of till and alluvium adjacent to the landslide, and of course, in the slide itself. A few glacial erratics of granite and related crystalline rocks occur in glacial deposits south of the landslide (Stops 1 and 2).

Description of the Landslide

The Slumgullion landslide is 6.8 km long, covers an area of 4.64 km^2, and has an estimated volume of $170x10^6$ m^3 (Parise and Guzzi, 1992). It consists of a younger, active, upper part that moves on and over an older, much larger, inactive part (Fig. 4). Recently, Williams and Pratt (1996) conducted seismic reflection and refraction surveys across the inactive part directly above Colorado Highway 149. They concluded that it occupies a broadly U-shaped valley cut into dense volcanic bedrock (5.4 km/s seismic velocity), and has a maximum thickness of 95 m. The active part of the landslide is 3.9 km long, covers an area of 1.46 km^2, and has an estimated volume of $20x10^6$ m^3 (Parise and Guzzi, 1992). Total elevation difference from the toe of the inactive part at the Lake Fork of the Gunnison River to the top of the 250-m-high scarp is about 1000 m (3400 ft). The length from the top of the scarp to the inactive toe at the level of the Lake Fork is about 6 km (3.6 mi). Part of the inactive toe is concealed under the water of Lake San Cristobal, which has a maximum depth of 28.5 m at the upstream terminus of the landslide toe (Crandell and Varnes, 1961; more recent measurements indicate a maximum depth of 27 m, Schuster, 1996).

A variety of land forms exist at the surface of the landslide or resulted from its movement; these include scarps, lobes, hummocks, closed depressions, flank ridges, benches, and risers. The largest feature, besides the landslide itself, is the main scarp and bowl-shaped depression at the head of the slide (Fig. 4*B*). Within the active landslide, gently sloping benches hundreds of meters across are joined by intervening steep sections (risers) tens of meters high. Swarms of scarps, related to normal faulting, commonly occur on upper parts of the risers; individual scarps are 0.1-10 m high. Long ridges, tens to hundreds of meters long and 1-5 m high, occur at both flanks and within the landslide. Most ridges are associated with strike-slip faults, however a few within the landslide appear to have resulted from stream erosion. Lobate hummocks are common in areas of shortening where they are associated with thrust faults and buckle folds. A few irregular hummocks of unknown origin occur at various places on the surface of the landslide.

Deposits exposed on the surface of the landslide or directly attributable to landsliding include trains of volcanic boulders, gray, white, yellow, light brown, and maroon diamictons (landslide debris), tan alluvium and pond deposits, clay dikes, and extrusions; all largely derived from the volcanic rocks. The diamictons are largely derived from hydrothermally altered rocks and are rich in clay and silt.

Limited geotechnical test data on samples collected from the surface of the Slumgullion landslide indicates that the landslide matrix has high clay content, and can be expected to have low strength and low permeability. Chleborad and others (1996) tested samples collected at the landslide surface of commonly occurring yellow, and reddish-brown, fine-grained materials that appear to form much of the matrix of the landslide debris. X-ray diffraction analysis detected only smectite in the yellow sample and both smectite and kaolinite in the reddish-brown sample. The yellow sample was also rich in gypsum. Particle-size analysis revealed that both samples were clay-rich (<0.002 micron), the yellow material had 58 percent clay, and the red material had 36 percent clay; the remainder consisted mainly of volcanic rock fragments. Both samples had high plasticity, the yellow material had a liquid limit of 95 and plasticity index of 50, whereas the reddish brown had a liquid limit of 65 and a plasticity index of 39. Both had high swelling potential and low in situ undrained shear strength (vane shear method).

We found tabular dikes of highly plastic clay (liquid limit = 110, plasticity index = 75) intruded into the landslide debris at several locations in the active landslide, notably along the strike-slip faults at the flanks (Fig. 3*B*) (Baum and Fleming, 1996). Similar intruded dikes were reported in the Twin Lake landslide in Utah by Fleming and Johnson (1989). Evidently the clay intrudes the faults during landslide movement. This clay is apparently much weaker than the rocky landslide debris on either side of the fault and intrusions of clay dikes along fault zones could facilitate continued movement by creating a weak, slippery (low angle of internal friction) layer between the active landslide and underlying materials. Creation of such a weak layer could permit the landslide to move in response to smaller loads or pore pressures than existed at the time of its initiation or reactivation.

Because of its size and inaccessibility, no quantitative hydrologic data exist for the Slumgullion landslide. The few available data indicate that the landslide is largely water saturated. Many ephemeral streams flow down the landslide and perennial streams flow down each flank. Perennial springs exist at several points on the surface of the landslide. Discharge from some of these springs appears to be several liters per second. Water from some of these springs flows hundreds of meters across the landslide before it either soaks into the ground or joins a stream. The relationships between surface and subsurface water, and the topography, structure, and stratigraphy of the landslide are complex, however, we infer from the abundance of surface water that a significant part of the active landslide is water saturated. Williams and Pratt (1996) concluded,

based on seismic reflection and refraction surveys, that even the inactive landslide debris is water-saturated several meters below the ground surface.

Although the active part of the Slumgullion landslide moves continuously, its rate of movement varies in both space and time. The maximum rate, about 6-7 m/yr, occurs at the narrowest part of the landslide and the rate decreases gradually upslope and downslope from that point as the landslide gradually widens (Fig. 5*A* and 5*B*). The average rate at the toe is 1-2 m per year and the average rate at the head is a few decimeters per year (Baum and Fleming, 1996). This pattern of displacement increasing from a minimum value at the head of a landslide, increasing to a maximum, and decreasing again to a minimum value at the toe is typical of landslides where we have information on displacement (Fleming and others, 1993; Baum and others, 1993; Baum and Fleming, 1991). The rate of movement also varies annually, with the fastest movement occurring during the latter part of and directly following the spring thaw and the slowest rate occurring just before the spring thaw (Savage and Fleming, 1996).

Several different lines of evidence indicate that the Slumgullion landslide has moved in at least three separate episodes. Crandell and Varnes (1960, 1961) recognized an older stable deposit and a younger, active landslide. Subsequently, Chleborad (1993), recognized that there were at least three different major episodes of landslide movement and dated the oldest unit on the basis of morphology, stratigraphy and radiocarbon ages. Madole (1996) also recognized and dated landslide deposits of at least three different ages at Slumgullion on the basis of morphology, stratigraphy, differences in degree of weathering and soil formation, and radiocarbon ages. During our mapping of the active landslide, we observed possible evidence for additional episodes. One of these is collapse of part of the main scarp that appears to have triggered the active slide. We will see and discuss some of the evidence for these episodes of movement during the field trip.

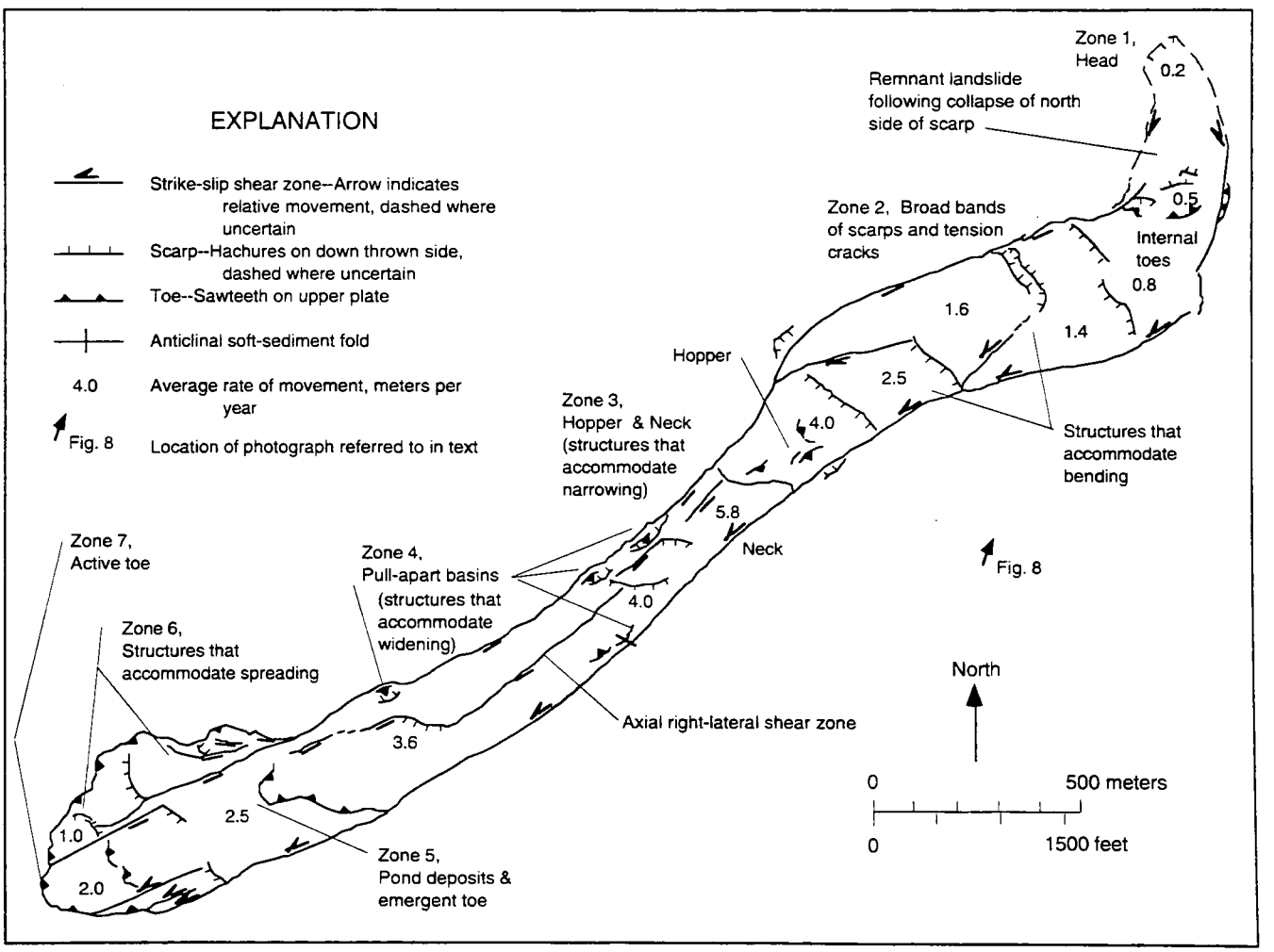

Figure 5A. Summary map of principal landslide elements. Map showing main kinematic features of the active landslide.

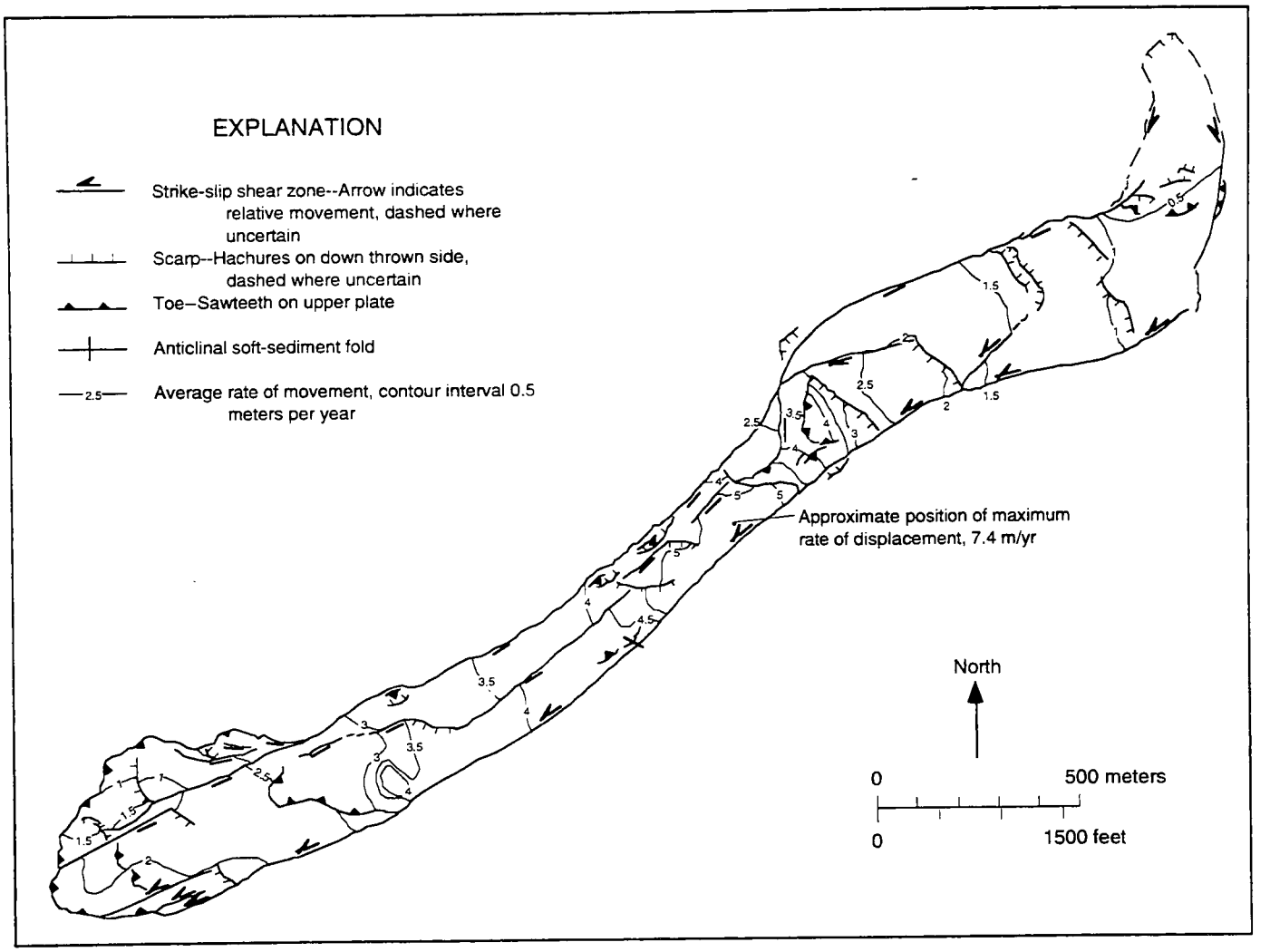

Figure 5*B*. Contours of annual displacement in meters, displacement data from Smith (1993). Contour interval 0.5 m, maximum rate 5 m/yr. Insufficient data to draw contours in neck where displacement locally exceeds 7 m/yr.

The oldest known unit (1.1-1.6 ka or perhaps older, Madole, 1996; Chleborad, 1996), recognized only in the upper part of the slide area, forms lobes and flank ridges that are as much as 30 m higher than younger flank ridges that lie inboard of the older features (Fig 4*A*). The soil developed on the oldest landslide unit is thicker than soil on the younger units and generally has a B horizon, whereas the soils developed in the younger two units lack B horizons or have incipient B horizons (Madole, 1996). The middle unit (probably 0.8-0.9 ka, Madole, 1996) crosscuts the oldest unit (Chleborad, 1993) and apparently extended farther downslope than the oldest unit, reaching the Lake Fork of the Gunnison River and damming it to form Lake San Cristobal. Soil of the middle unit has been partially eroded and consists of an A horizon developed on slightly oxidized parent material. The presently active part of the Slumgullion landslide is the youngest unit (0.3 ka, Crandell and Varnes, 1960, 1961). The only recognizable soil on the active slide is relict soil developed on blocks of older landslide deposits that have been incorporated into it.

FIELD-TRIP ROAD LOG

Mileage cum.	Mileage inc.	
0.0	0.0	Trip starts in Lake City at intersection of Second Street (Henson Creek/Engineer Pass Road) and Colorado State Highway 149. Drive south on State Highway 149.
0.1	0.1	Cross Henson Creek
2.5	2.4	Cross Lake Fork of the Gunnison River. Yellow deposits to right are downstream limit of Slumgullion landslide deposits (middle unit of Madole (1996), 0.8-0.9 ka).
4.1	1.6	Cross north flank of Slumgullion landslide deposits (middle unit of Madole (1996), 0.8-0.9 ka). Highway 149 traverses inactive part of slide for next 0.4 mi.
4.5	0.4	Parking area to left is where field vehicles will meet us at end of trip.

Mileage cum.	inc.	
4.5	0.0	Cross south flank of Slumgullion landslide deposits, enter area underlain by glacial deposits and volcanic bedrock.
5.0	0.5	**STOP 1. HIGHWAY 149 SCENIC OVERLOOK OF LAKE SAN CRISTOBAL AND THE SLUMGULLION LANDSLIDE.** Parking area at switch back in Highway 149. View Lake San Cristobal to southwest, toe and inactive deposits of Slumgullion landslide to west and northwest. View up axis of active part of Slumgullion landslide to northeast. Return to Highway 149 and continue uphill (east).
6.0	1.0	**STOP 2. SLUMGULLION LANDSLIDE SCENIC OVERLOOK.** Turn left into parking area on north side of highway 149. View part of the active Slumgullion landslide to north. Slumgullion Creek is in valley between parking area and landslide deposits. Return to Highway 149 and continue uphill (east).
6.8	0.8	For next 0.4 mi., Highway 149 makes broad loop around remnant toe of the Slumgullion landslide that blocked Slumgullion Creek (oldest unit of Madole (1996)).
7.6	0.8	Yellow and white deposit to left is part of an ancient spill-over of the Slumgullion landslide (oldest unit of Madole (1996)). Radiocarbon age of wood found in these deposits in 1992) ranged from 1.1-1.6 ka (Chleborad, 1993, 1996).
8.1	0.5	Windy Point Overlook
9.3	1.2	Turn left, go north past campground on gravel road.
10.2*	0.9*	Turn left onto 4WD trail (must have special permission from U.S. Forest Service and good weather/road conditions to drive up trail beyond this point). Follow 4WD trail to edge of east scarp at top of Slumgullion landslide.
10.8*	0.6*	**STOP 3. MAIN SCARP OF THE SLUMGULLION LANDSLIDE.** Look west and behold the breathtaking (maybe its just the altitude!) view of the Slumgullion landslide. Hike down scarp onto landslide, and then hike down slide to active toe. Driver(s) will take field vehicles to parking area below active toe and await our return.

* Mileage estimated from USGS topographic map

STOP 1. HIGHWAY 149 SCENIC OVERLOOK (SWITCH BACK)

At this stop we will view Lake San Cristobal (Fig. 4*B*), and most of the Slumgullion landslide (Fig. 6). Lake San Cristobal, Colorado's second largest natural lake, formed about 800-900 years ago when the Slumgullion landslide dammed the Lake Fork of the Gunnison River. Originally the lake was 4.3 km long, and had a surface area of 1.8 km^2, but sediment deposited in deltas of Slumgullion Creek and the Lake Fork have reduced the lake's length to 3.3 km and its area to 1.34 km^2. The lake is 27 m deep and has a volume of approximately 14 million m^3 (Schuster, 1996). The landslide buried the original channel of the Lake Fork and the river eventually cut a new channel around the perimeter of the landslide toe 200 m west of and 28 m higher than the old channel. The new channel, which originally formed because the low point in the landslide-dam crest was against the west wall of the valley, has cut down about 10 m into resistant bedrock forming a stable, erosion-resistant channel. Headward erosion of the downstream channel has created 25-m-high Argenta Falls at a resistant bedrock ledge (Schuster, 1996).

Much of the toe of the inactive landslide is visible from this point (Fig. 4*B*). The toe spread laterally both up- and downstream when it reached the Lake Fork of the Gunnison River. The total width from the upstream end (submerged) to the downstream end is 2.8 km. The lower part of the landslide rises from the toe to the crossing of Highway 149 through a series of steps (Parise and Guzzi, 1992). It is not known whether these resulted from steps in the original bedrock channel of Slumgullion Creek or if they are depositional structures in the landslide debris itself.

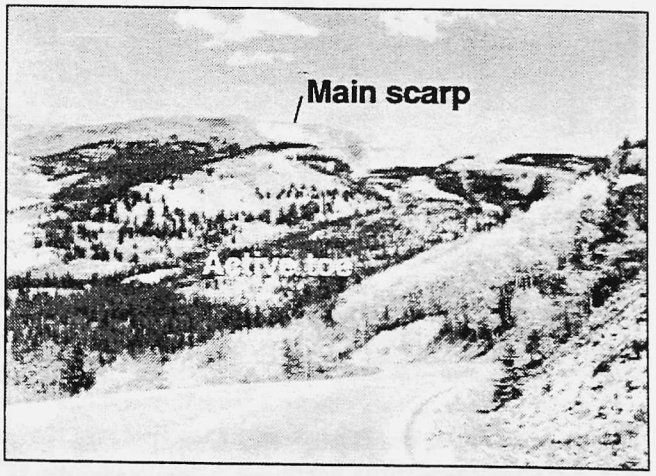

Figure 6. Active part of the Slumgullion landslide, view to northwest from Stop 1 (photograph by Jack Odum, U.S. Geological Survey).

STOP 2. SLUMGULLION LANDSLIDE SCENIC OVERLOOK (PULLOUT)

Here we have a view across the lower part of the active landslide (Fig. 7). The west part of the main scarp is visible in the distance (Fig. 7*A*) as are inactive flank ridges on the south side of the landslide. The active shear zone, on the south side of the landslide where continuous slip monitoring of bounding strike slip faults (Savage and Fleming, 1996) and detection of slidequakes (Gomberg and others, 1995) was carried out can be seen to the northeast (Fig. 7*A*). A smaller landslide superposed on the active Slumgullion landslide is visible to the north (Fig. 7*A*). Extensive pond deposits on the active landslide can be seen to the northwest (Fig. 7*B*). The uphill end of these deposits marks the location where Parise and Guzzi (1992) postulated that the toe emerged about 300 years ago.

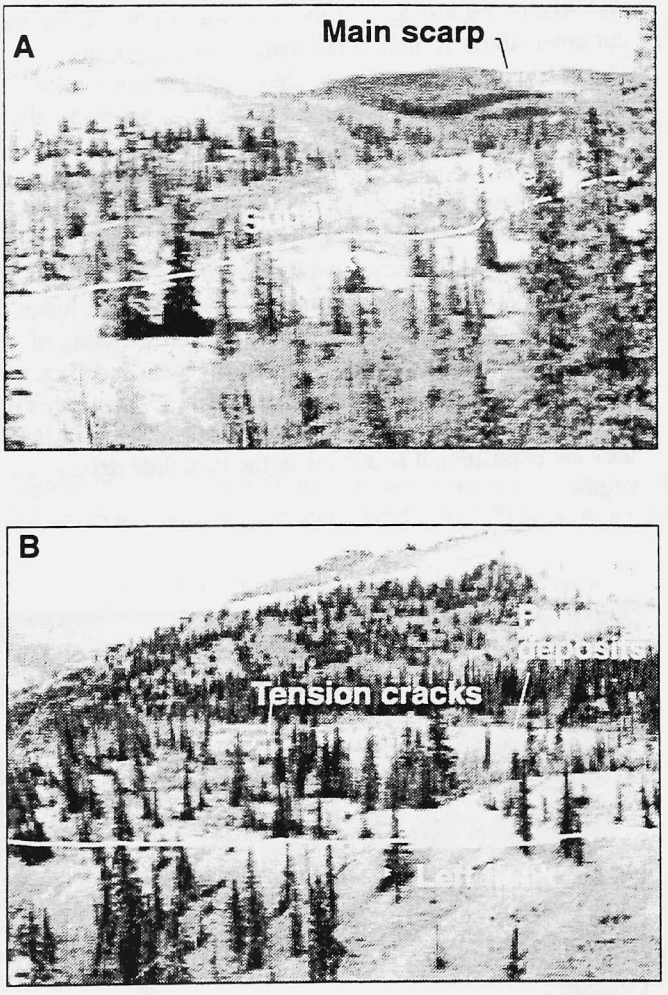

Figure 7. Views of the Slumgullion landslide from Stop 2. *A.* Looking toward the northeast, a smaller landslide superimposed on the active Slumgullion landslide is shown at the center of the photograph. *B.* Looking north-northwest, extensive pond deposits on the active landslide are visible near the center of the photograph.

STOP 3. SLUMGULLION LANDSLIDE

This stop provides a magnificent view of the setting of the Slumgullion landslide and involves a hike from the main scarp downslope to the active toe. We plan to make several stops along the way to examine specific landslide features. Landslide features described in the text are referenced to alphabetically labeled points on the maps to aid the reader in locating the features. The right and left flanks of the landslide are defined from the viewpoint of someone looking downslope along the axis; the left flank is the south side and the right flank the north side. If the reader wishes to locate a specific feature, positions are given with respect to the alphabetical stations and some specified distance from a given flank. Maps of adjoining areas overlap and the alphabetical stations in areas of overlap appear on both to aid the reader in comparing the maps.

We will be examining the main scarp, various parts of the active landslide, and deforming ground ahead of the active toe. The active landslide can be divided into seven zones based on similarity of structural features within each (Fig. 5*A*). The uppermost, Zone 1, is called the *head*. It contains fractures indicative of both stretching and shortening. Downslope from the head is Zone 2, *broad bands of normal faults and tension cracks*, that is more than 600 m wide. The next zone (3), the *hopper and neck*, is a funnel-shaped stretch where the landslide has its minimum width and the displacement rate reaches its maximum. Downhill from the hopper and neck, the landslide gradually increases in width through curves or offsets in the flank faults creating Zone 4, *pull-apart basins along both flanks*. The next principal features are (Zone 5) *pond deposits and an emergent toe* followed by an area of *shortening and spreading* (Zone 6), and Zone 7, the *active toe*. In general, the upper part of the landslide (Zones 1 and 2) is characterized by features associated with stretching such as normal faults and tension cracks. The lowermost part of the landslide (Zones 5, 6, and 7) is characterized by features associated with shortening such as thrust faults. In between (Zones 3 and 4), features are a result of widening or narrowing of the landslide. Also, in places where the slope of the landslide is locally steeper than average, small landslides form on the surface of the larger landslide (Fig. 7*A*).

MAIN SCARP AND SOURCE AREA

The materials exposed in the main scarp are a complex array of hydrothermally altered and unaltered volcanic materials including tuffs and intrusive and extrusive rocks of variable composition (Diehl and Schuster, 1996). The Miocene Hinsdale Formation at the top of the 230-m-high scarp is unaltered vesicular basalt (Fig. 8). Below the basalt is the Miocene Sunshine Peak Tuff, a welded ash flow tuff. These Miocene units unconformably overlie the highly altered Oligocene Uncompahgre Peak volcanics, which consist mainly of andesite flows (Lipman, 1976). The products of hydrothermal alteration, including alunite, smectite,

and opal, have been found in the altered rocks of the main scarp as well as the debris forming the slide (Larsen, 1913; Diehl and Schuster, 1996). Faults, breccia pipes, jointing, and alteration contribute to the instability of the main scarp, and rock avalanche chutes coincide with many of the faults (Diehl and Schuster, 1996).

There is a general variation in composition of the main scarp that has been useful in correlating landslide deposits with their sources. Rocks exposed on the south side of the main scarp are almost entirely altered to clays and range in color from nearly white through yellow, brown, and red. There is a conspicuous lack of resistant, unaltered intrusive or extrusive rocks to contribute to the landslide deposits. The form of the scarp also is different on the south side. Here, the top of the scarp is a north-trending topographic divide, and the ground slopes away from the scarp in both directions indicating that the uppermost part of the landslide broke through the crest of a hill. We will cross the south part of the scarp to get onto the landslide. On the north part, the scarp is not a topographic divide but rather the ground slopes down from Mesa Seco to an abrupt break in slope at the top of the scarp. Rock in the northerly part of the scarp is capable of contributing large quantities of resistant, slightly altered to unaltered rocks to the landslide deposits.

Zone 1—Head

The uppermost fractures that we mapped in the head of the landslide form a narrow zone on a topographic bench below a large pile of coarse talus (Area below ***B*** in Fig. 8 and near **A-A'**, Fig. 9). The fractures are poorly expressed tension cracks and normal faults; both indicative of stretching. The landslide material in the area of the fractures is a powdery clayey silt that does not preserve fractures well. The scarps of the normal faults are low and some face uphill; others face downhill. Several features that have the appearance of sinkholes and long, linear furrows are interpreted to be depressions above tension cracks that opened at depth and propagated to the surface as collapse features. The band of most active features, near **A-A'**, is about 100 m across the landslide and about 20 m wide in the direction of sliding. The stretching rate as measured across the zone of fractures is about 0.2 m/yr. The flanks of the landslide downhill from the stretch fractures are obscure, but several segments of an active strike-slip fault are preserved along the left flank about 70 m downhill. Other than these few faults, the flanks were located (Fig. 9) by a change in slope or small furrow. Movement rates are apparently insufficient to maintain a conspicuous set of fractures.

Figure 8. West part of main scarp, looking north. Collapse that triggered present episode of movement evidently came from area labeled A. Head of active slide directly below point B. Main body of active slide in strip of tilted evergreens in middle of photograph. Axis of active slide curves abruptly from south (roughly toward viewer) at head to west (toward viewers left) near center of photograph.

The direction of sliding at the head is toward the south and is in the same direction as the inferred collapse of the Mesa Seco (Fig. 4*A* and 5*A*). The load produced by the collapse apparently was the trigger for the currently active landslide (Fig. 5*A*). Remnants of the toe of this collapse are preserved as linear ridges outside the left flank in the vicinity of **C'** and within the active landslide along a discontinuous zone of toes about 70-90 m downhill from the line **C-C'** (Figs. 9 and 10). Uphill from the toes, in the area of **C-C'**, is another zone of stretch features much like the uppermost zone mapped at **A-A'** and consisting mostly of uphill facing scarps as much as 1.5-m high (Fig. 10). The mixture of stretch features produced by normal faults and tension cracks in the active landslide contrast sharply with the compressional features produced by collapse of part of the main scarp (Fig. 9) in the same general area.

The presence of compressional and extensional features at the same places is confusing and alternative explanations for their coexistence are plausible. The uppermost stretch features are at **A-A'** (Fig. 9). Principal shortening features are along a line between **D** and **C'**. Here, a zone of discontinuous internal toes and trees that have been pushed over and partly overridden by landslide material are diagnostic of shortening. Overlapping the shortening features is a band of stretching features, principally scarps of normal and oblique-slip faults, that loosely connect with the north (right) flank. The stretch faults are probably a continuation of the zone of normal faults that intersect the right flank between **D** and **E**. The toe of the small landslide between **A-A'** and **D-C'** is being pulled apart by more rapid movement along the right flank farther downhill.

Displacement rates in the head of the landslide are small and the southward movement in the head of the landslide is nearly independent of the westward movement farther downslope. The value of 0.2 m/yr at the uppermost fractures is a minimum because measurement points did not extend across all the fractures. Farther downslope, at a point on the left flank about 25 m uphill from line **C-C'** movement was only 0.1 m/yr. On the right flank, a point

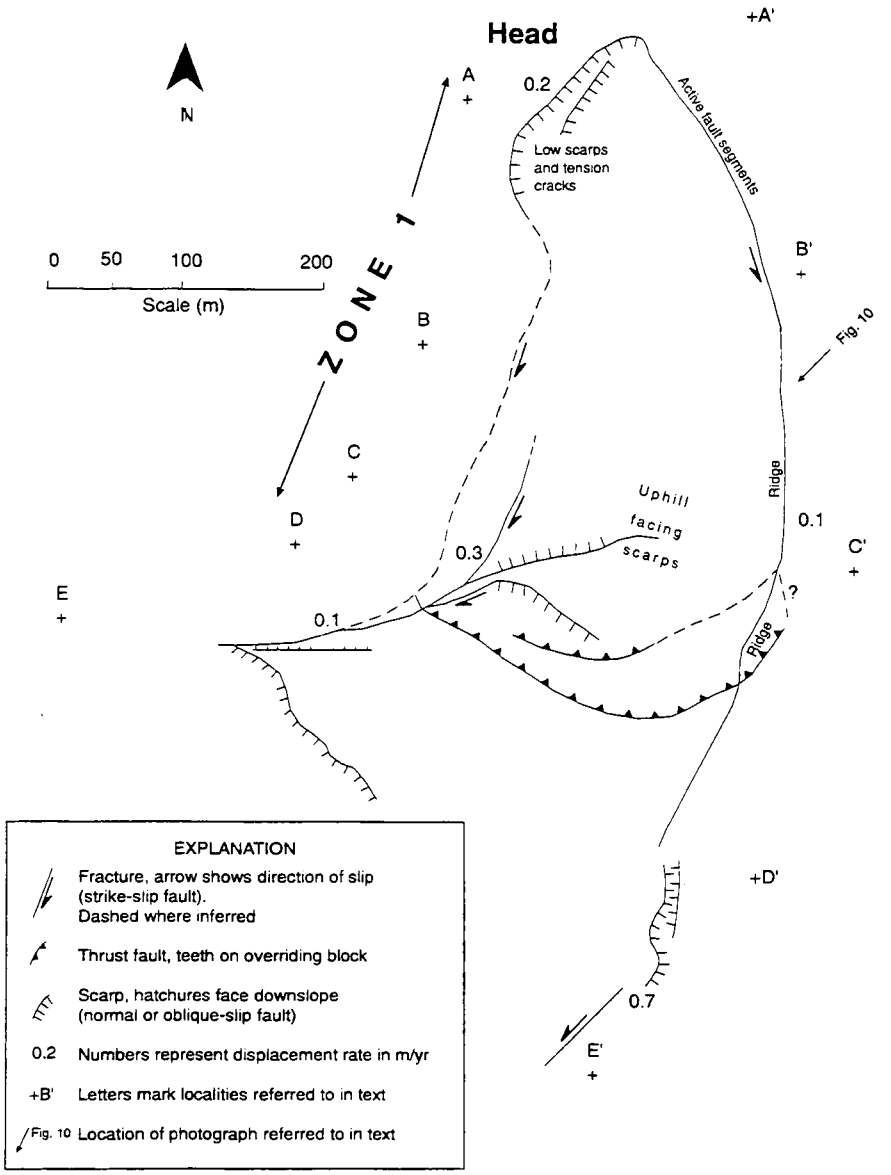

Figure 9. Simplified map of deformational features in Zone 1, Head.

near line **C-D'** was displaced 0.3 m and a point 110 m downhill from there and due south of **D** was displaced 0.1 m/yr. These few measurements indicate remnant displacement in the form of a separate, discrete landslide that resulted from a previous episode of main-scarp failure. Indeed, we were unable to find continuous fracturing along the left or right flank directly uphill from **D-D'**, and the interior of the landslide in the vicinity of **D-D'** has very few fractures of any type that would connect the small landslide between **A-A'** and **D-C'** with the larger active landslide farther downslope.

Zone 2—Broad Bands of Normal Faults and Tension Cracks

Fracturing that is more typical of the head of a landslide than that described from Zone 1, are found in the three broad bands of normal faults and tension cracks of Zone 2. Fractures are similar in each of the bands and occupy a reach of the landslide that is nearly 1 km long and is characterized throughout by stretching or extension. Included are normal faults with scarps facing both uphill and downhill, tension cracks oriented approximately at right angles to the direction of sliding, and stretched roots/split trees with the stretch direction parallel to the direction of sliding. Figure 11 summarizes the main structures and shows annual displacement for a few selected points within and on the boundaries of the landslide.

The scarps and other stretching features are concentrated in three distinct bands. The uppermost band, which intersects the boundary near point **C** on the north side of the landslide contains normal faults in a 200-m-wide band that only goes part way across the landslide. This band, at **C-D'**, extends through the toe of the landslide deposit from collapse of the main scarp (at *A* in Fig. 8). This band occurs at the abrupt 90 degree clockwise bend in the landslide. Displacement is 0.3 and 0.7 m/yr on the north and south sides of the landslide respectively. This uppermost band contains a right-lateral, strike-slip fault on the north side that carries almost the entire displacement on the right flank (north side, Fig. 11). The strike-slip fault is loosely connected with the poorly developed normal faults and tension cracks that extend part way across the landslide. Boundary fractures farther to the north appear to be inactive or the landslide is moving too slowly there to maintain open fractures.

The middle band of stretching features extends across a broad area between **E-E'**. This band extends entirely across the 350-m-wide landslide; the band extends downhill at least 250 m on the north flank and 100 m on the south flank. Individual scarps do not extend all the way across the landslide, but rather they occupy the band as many individual, overlapping normal faults and tension cracks. Scarps of the normal faults range in height up to

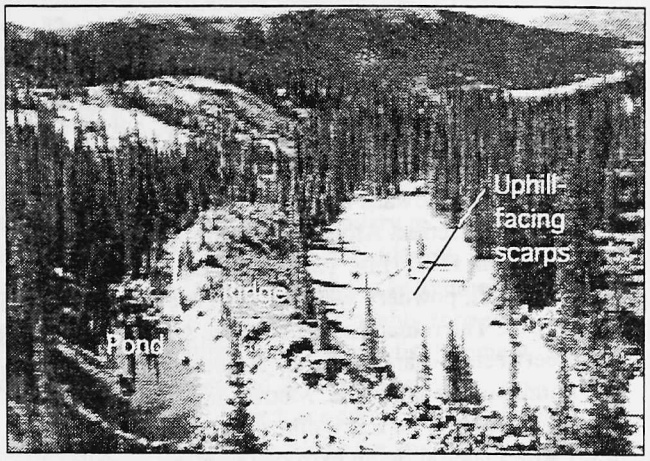

Figure 10. View to south-southwest of flank ridge and uphill facing scarps near 90°-bend in landslide (downhill end of Zone 1).

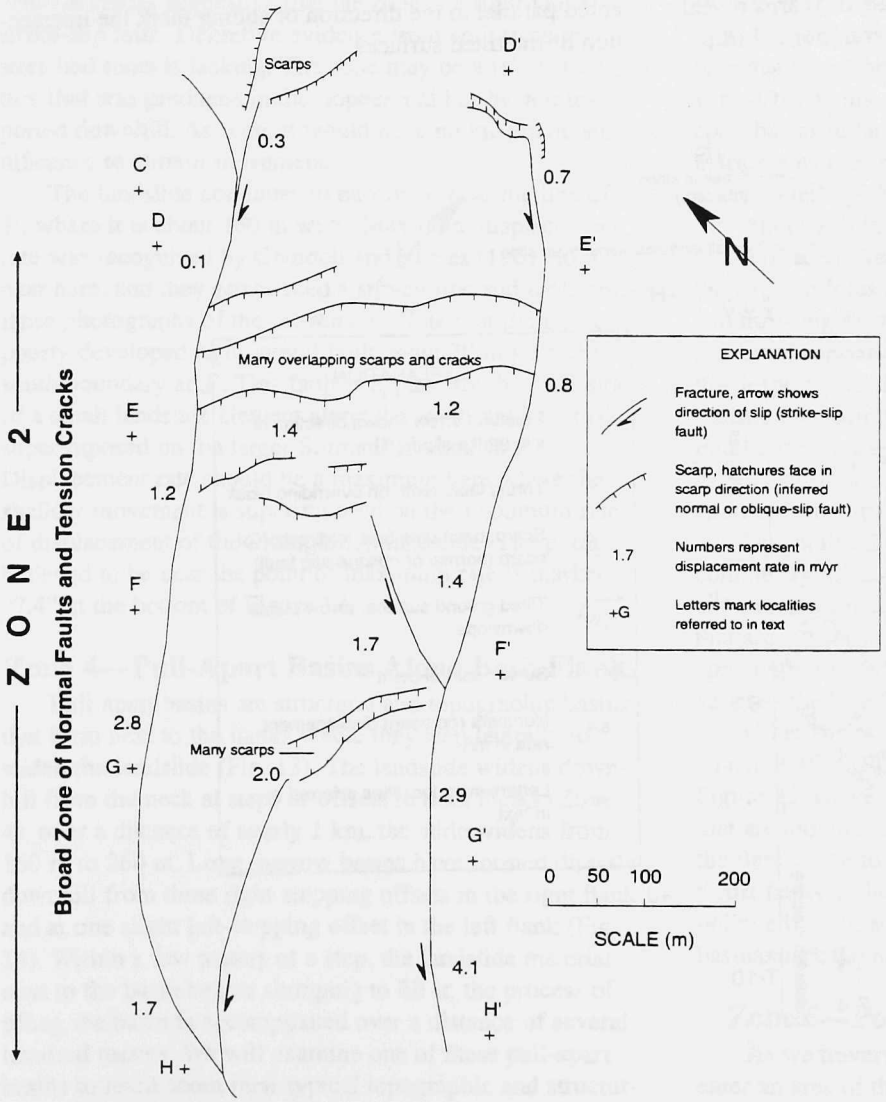

Figure 11. Simplified map of deformational features in Zone 2, Broad Bands of Normal Faults and Tension Cracks.

about 2 m. Displacement at a point 95 m uphill from **E'** on the left flank is 0.7 m/yr and increases to 0.8 m/yr at a point 110 m downhill from **E'**. On the north flank, 40 m downhill from E, displacement is 1.2 m/yr.

The difference in displacement of about 0.4 m/yr on the north flank compared to the south flank of the landslide has kinematic significance, because it must be accommodated either by internal distortion or by movement on one or more fault zones. The normal faults and tension cracks terminate in a well defined, left-lateral strike-slip fault zone (near **F'**, Fig. 11) that carries about 0.3 m of the displacement difference between the landslide flanks. The left-lateral fault and adjoining band of normal faults define a block that can move through the 20° bend near **F'** with relatively little internal distortion, because the block is free to move nearly parallel to the flanks downhill from the bend.

The third band of normal faults extends between **F'-H**. Here, scarps and fractures are in a band more than 50 m wide that transforms into a right-lateral, strike-slip fault where the band narrows midway across the slide near **G**. The strike-slip fault approaches the north flank near **H** (Fig. 11). Displacement rate along the north flank is 2.8 m/yr near **G** and declines to 1.7 m/yr near **H**. Meanwhile, displacement increases along the south flank from 2.9 m/yr near **G'** to 4.1 m/yr near **H'**. Apparently, there is more than 2 m/yr of displacement across the internal strike-slip fault. The position of this band also corresponds to a sharp bend in the landslide; it turns counterclockwise 30° directly upslope from **H**.

The three internal strike-slip faults evidently accommodate movement through curves in the flanks. Each of the broad bands of normal faults has an associated strike-slip fault that joins the band to the flank where it curves. Overall, displacement progressively increases downslope from less than 0.1 m/yr to nearly 3 m/yr over the length of the zone.

Zone 3—The Hopper and Neck

The hopper is a 150-m-long funnel-shaped area in the 500-m-long zone termed Hopper and Neck that accommodates narrowing of the landslide. The width of the landslide decreases from 230 m at **H-H'** to 180 m at **I-I'**, over the 150 m horizontal distance.

The hopper begins downhill from the third band of normal faults and tension cracks described above (Fig. 11)

and extends 500 m downslope to the narrowest part of the landslide, the "neck". The materials entering this narrowing part of the landslide are constrained laterally and materials have the appearance of entering a hopper. We will cross an abrupt change in slope as we enter the hopper. Fig. 12 is a simplified map of fractures and other features in the hopper.

On the north side of the landslide, 30 to 50 m downhill from **H**, the landslide surface has been tilted toward the center (indicated by "tilt" with arrows on Fig. 12). This tilted area is matched for symmetry by a tilted surface on the south side that extends a little farther downslope than on the north side. The slope of the tilted surface on the north side is as much as 50 percent ($(\Delta v/\Delta h)\times 100\%$) whereas tilt amount on the south side is smaller, as much as 20 percent. The tilted surface on the north side is terminated on its downslope end by a discontinuous line of scarps that extends from the north flank near **H** obliquely toward **I'**. Small *en echelon* tension cracks in the line of scarps reveal that the sense of slip is oblique, a left-lateral, normal (dip slip) fault zone.

Trees on the tilted surface on the north side are uniformly inclined toward the middle of the landslide and are approximately normal to the ground surface; trees are generally absent on the south side. The tilted surfaces are inclined toward each other, and the inclined surfaces progressively point toward the middle of the landslide in a downslope direction. Along both flanks of the landslide, from **H-I** and **H'-I'** (Fig. 12), the landslide debris is void of trees and soft, powdery white-to-yellow clay-rich material is exposed. The remaining trees on the surface of the landslide between **H-I** are along the bottom of the swale down the middle of the landslide. Motion on each flank of the hopper appears to be screw-like (in transverse cross section) with material being extruded near the landslide flanks and being folded together along the midline of the landslide. Landslide materials are extensively remolded in the short stretch between **H-H'** and **I-I'**. The hopper-like structure ends approximately at **I-I'** where two thrust faults oriented parallel to the direction of sliding mark the intersection of the tilted surfaces.

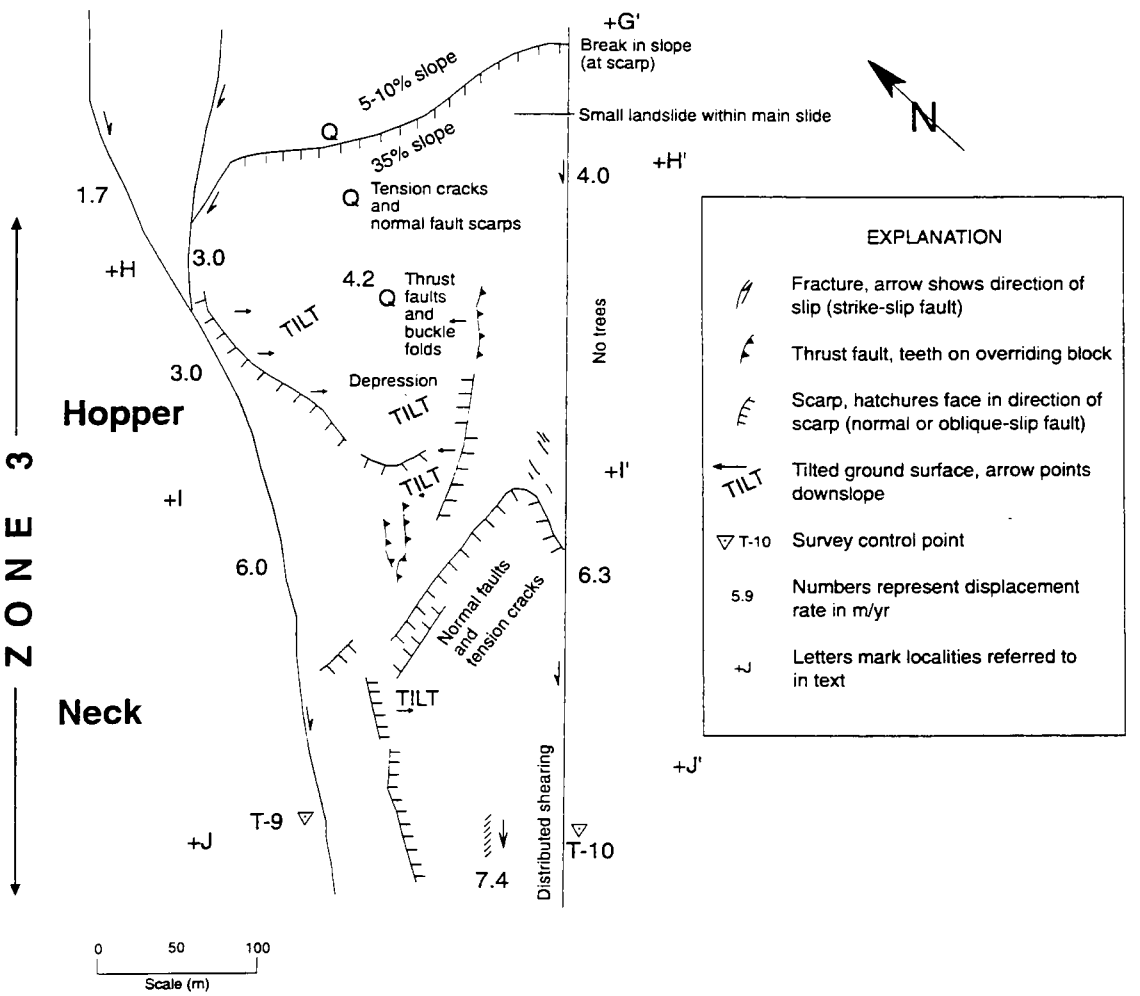

Figure 12. Simplified map of deformational features in Zone 3, Hopper and Neck.

The downslope end of the hopper-like structure is abruptly broken by a sharp zone of normal faults and tension cracks. The zone begins at **I'**, trends obliquely downhill across the landslide toward **J**, turns north and intersects the north boundary of the landslide halfway between **I** and **J**. Small *en echelon* tension cracks in the well-formed zone about 50 m inside the south boundary at **I'** indicate that slip is oblique, right-lateral and normal (down). Most of the narrowing of the landslide has been accommodated farther upslope, and this structure has probably formed to accommodate a continuation of increasing displacement rate with distance from the head of the landslide.

There is a line of fractures and scarps that trends downslope from the place where the zone of normal faults and tension cracks changes direction (halfway between **I** and **J**, 50 m from the north boundary). This line continues roughly parallel to the landslide boundaries. The features along the line are not well preserved; locally, there are *en echelon* cracks suggestive that the zone is a right-lateral strike-slip fault. Definitive evidence from split trees or stretched roots is lacking. The zone may be a relict structure that was produced in the hopper and has been transported downhill. As such, it would have no kinematic significance to current movements.

The landslide continues to narrow to near the line of **J-J'**, where it is about 160 m wide. Maximum displacement rate was recognized by Crandell and Varnes (1961) to be near here, and they established a survey line and took time-lapse photographs of the movement. Note that there is a poorly developed right-lateral fault about 30 m from the south boundary at **J'**. This fault is apparently the right side of a small landslide element along the south flank that is superimposed on the larger Slumgullion landslide. Displacement rate should be a maximum here where the shallow movement is superimposed on the maximum rate of displacement of the Slumgullion landslide. The point believed to be near the point of maximum rate is marked "7.4" at the bottom of Figure 12.

Zone 4—Pull-Apart Basins Along Both Flanks

Pull-apart basins are structural and topographic basins that form next to the flanks where they step laterally to widen the landslide (Fig. 13). The landslide widens downhill from the neck at steps or offsets in both flanks (Zone 4); over a distance of nearly 1 km, the slide widens from 160 m to 260 m. Long, narrow basins have formed directly downhill from three right-stepping offsets in the right flank and at one slight left-stepping offset in the left flank (Fig. 14). Within a few meters of a step, the landslide material next to the basin begins slumping to fill it; the process of filling the basin is accomplished over a distance of several hundred meters. We will examine one of these pull-apart basins to learn about their typical topographic and structural features and the process of basin filling.

The best expressed basin is on the north side, between **J** and **K** in Figure 13; less well expressed basins on the north side are between **L** and **M** and between **M** and **N**. The well-developed basin between **J** and **K** contains all the features seen at the other basins and is depicted in Figures 15, 16*A*, and 16*B*. The zone of strike-slip faulting on the north (right) flank bifurcates where it changes orientation at J; one part follows the north flank as a narrow zone of strike-slip faulting on the landslide boundary (Fig. 15). The other part forms a crescent-shaped group of scarps and fractures that gradually turns parallel to the north flank (Fig. 16*A*). A 5-m deep basin occupies the area between this crescent-shaped group and the north flank. Within the basin and parallel to the landslide boundary, there are several shortening features such as small thrust faults and buckle folds. Rotated blocks bounded by the crescent-shaped group of scarps and the shortening features in the basin are smaller landslides within the overall larger landslide in which material is being transported into the basin (Fig. 15). The crescent-shaped group of scarps are the surface manifestation of oblique-slip (right-lateral- and dip-slip) listric faults. The structure appears analogous to pull-apart basins in larger tectonic settings where movement on listric faults transports material from the flanks of the basin to its center.

About 200 m downhill from **J**, the crescent-shaped group of scarps turns toward the basin and terminates in the basin in folds and thrust faults (Fig. 15). The buckling and thrusting is evident mostly in the tilting of small trees and bushes in the basin (Fig. 16*B*). There is a small pond at the deepest part of the basin that accumulates water-transported sediment and helps fill the basin (Fig. 16*A*). Pond sediments extend downslope from the existing pond as the landslide translates the materials, but not the pull-apart structure, downslope.

Downhill 50 m from **K** (Fig. 15), the basin has been completely filled. Further downhill from the basin, there are numerous inactive scarps and hummocky topography that are not shown on the sketches. These inactive features apparently formed in the pull-apart basin and were deactivated as they were transported beyond the basin.

Other basins along the active flanks of the Slumgullion landslide (Fig. 13) do not contain all the features shown on Figure 15. However, they do generally have slump blocks that are moving from the inboard side of the basin toward the flanks. The toes of these slumps form folds and/or thrust faults in the deepest parts of the basins. Likewise, oblique lines of scarps at the downhill ends of the larger basins mark the heads of these slumps that fill the basins.

Zone 5—Pond Deposits and Emergent Toe

As we traverse downhill from Zone 4 into Zone 5, we enter an area of thrust faults and extensive pond deposits. The area of thrust faults uphill from the pond deposits is centered approximately on **O-O'** and is the first major indi-

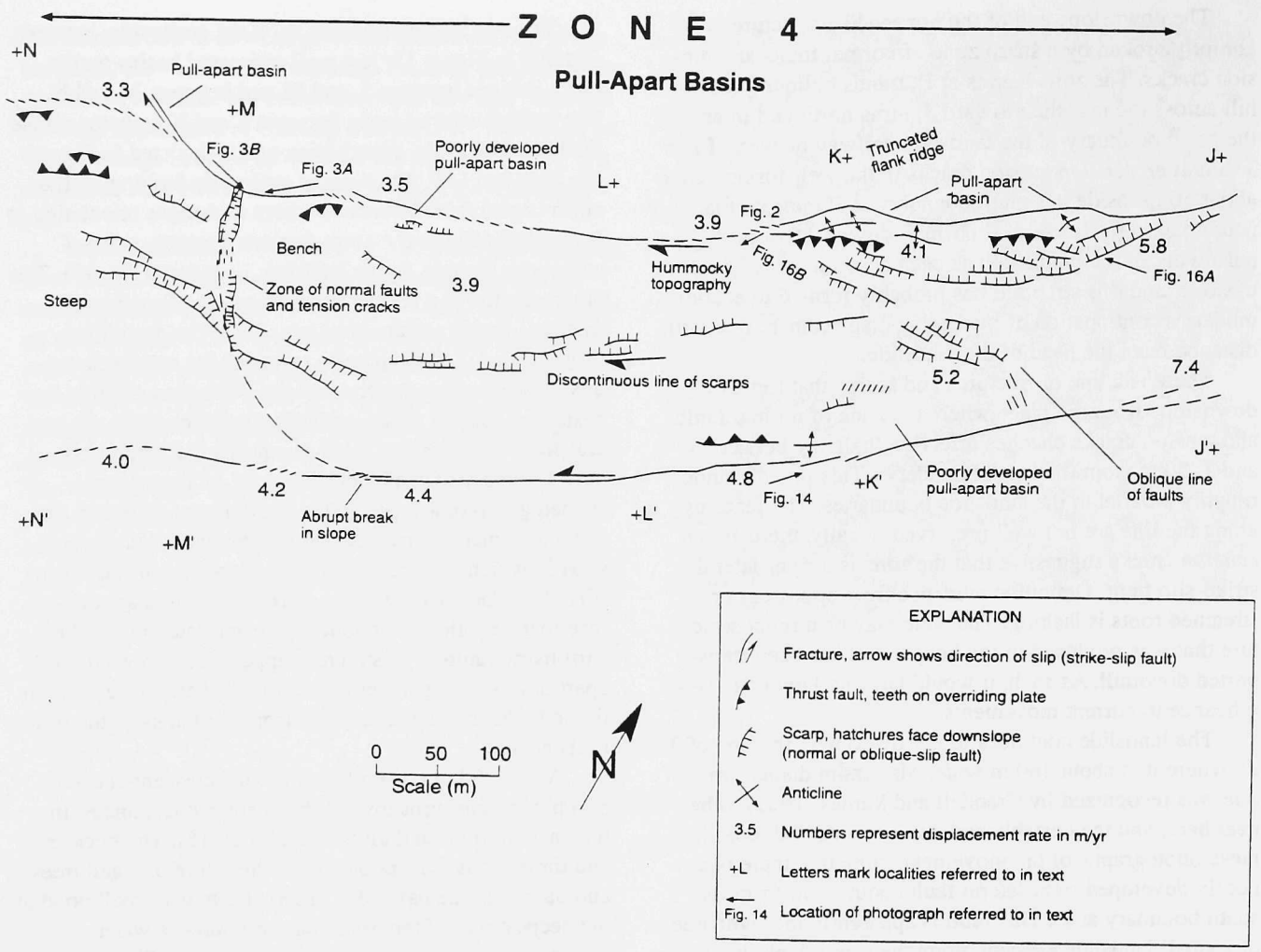

Figure 13. Simplified map of deformational features in Zone 4, Pull-Apart Basins Along both Flanks. Note steps or offsets in flanks directly upslope from the basins.

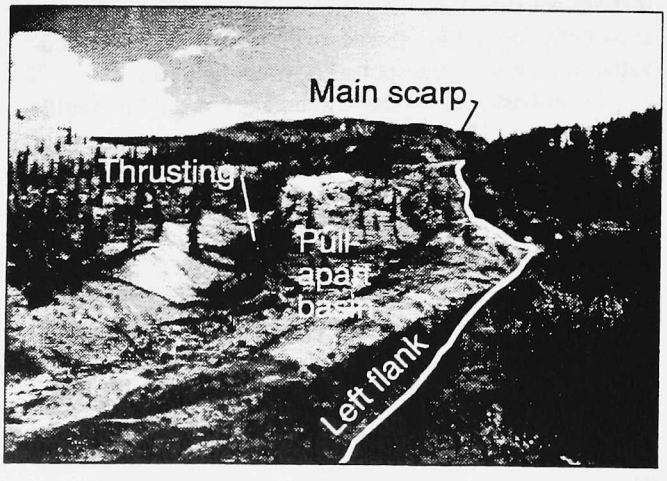

Figure 14. View of poorly developed pull-apart basin along left flank (photograph by Jack Odum, U.S. Geological Survey).

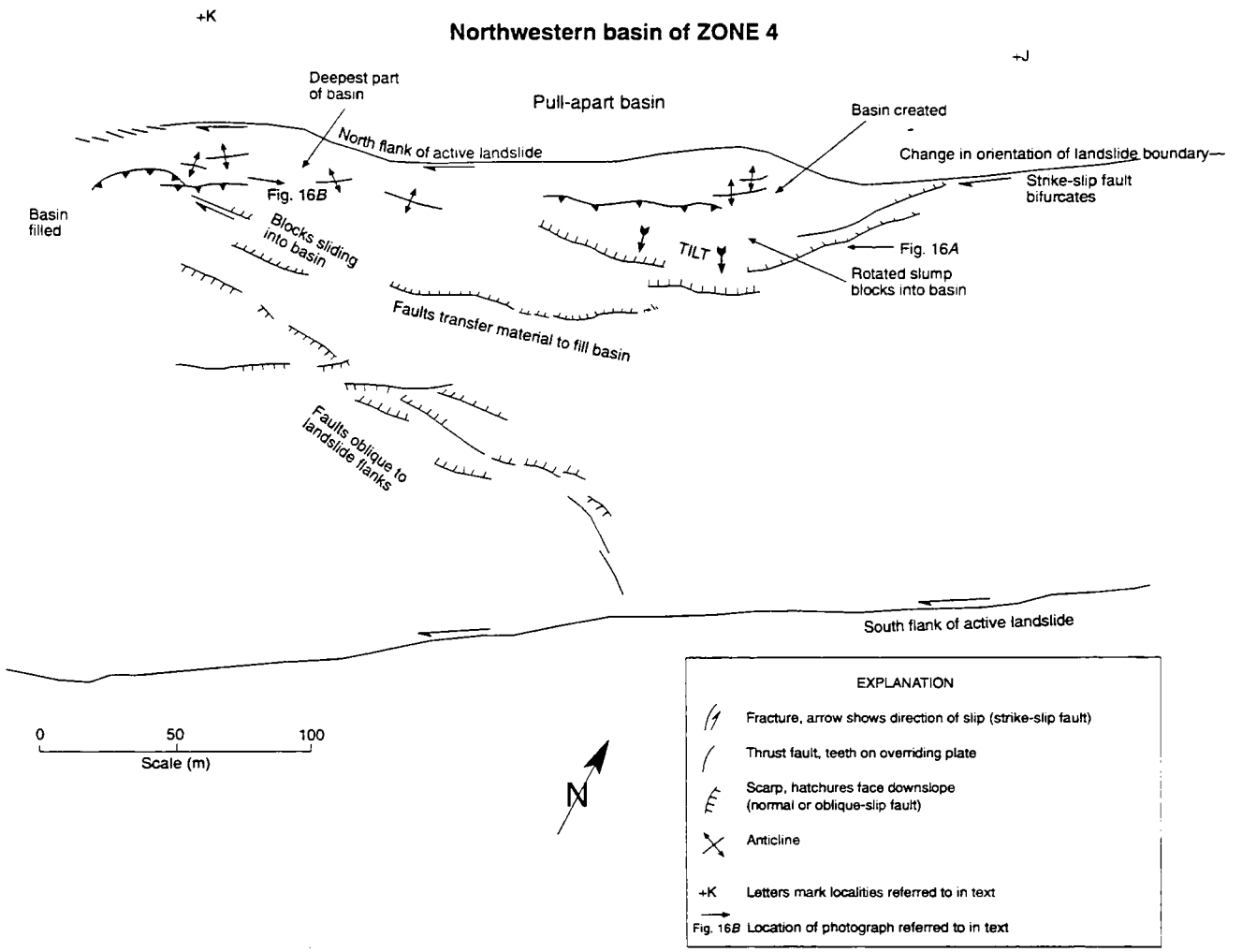

Figure 15. Idealized features in pull-apart basin based on the basin on the north flank between J and K. The basin forms where the landslide becomes wider through a bend or step in the bounding strike-slip fault. The features created within the moving landslide all serve to translate material into the basin. In the upper part, material is moved into the basin by a series of rotational slumps. Farther downslope, material is translated into the basin along curving strike-slip faults that terminate in the basin in buckle folds and thrust faults. At the downslope end of the basin, there is a zone of oblique slip faults that translate material across the landslide and complete filling of the basin.

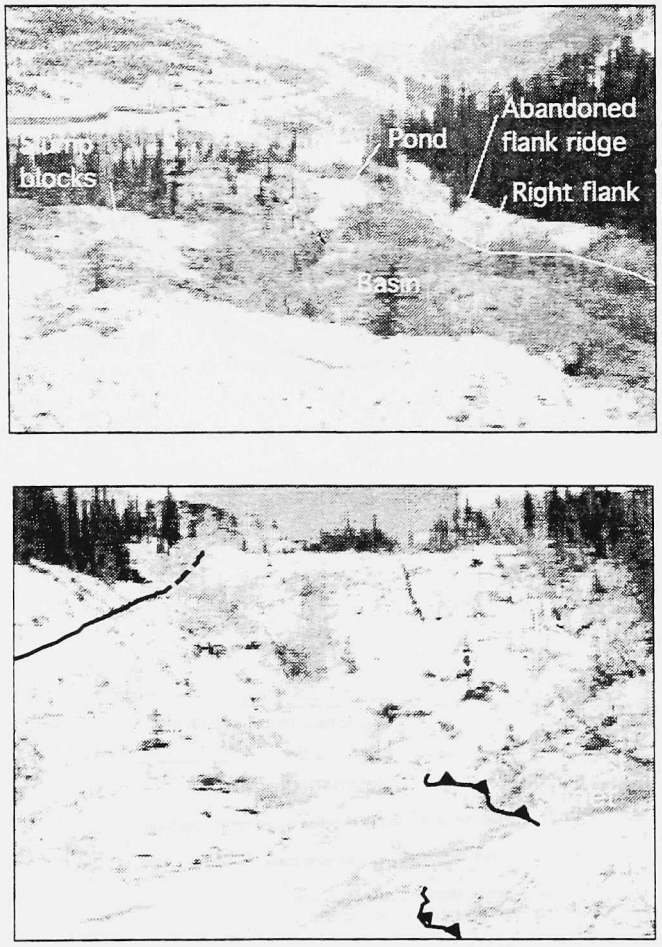

Figure 16. ***A.*** **View looking southwest into large pull-apart basin on right flank.** ***B.*** **View to northeast from bottom of same pull-apart basin, pond sediments in foreground. Note tilted trees on thrust sheet.**

cation of deep-seated shortening features on the landslide (Fig. 17). Other thrust faults uphill from this area are related to pull-apart basins or represent internal toes of small landslides superimposed on the larger landslide. Across the zone of thrust faults at **O-O'**, the displacement rate diminishes from about 4 m/yr to about 2.5 m/yr. The position of this zone of shortening coincides with a large, inactive segment of landslide toe to the north of the active landslide flank at **O**. This inactive part of the toe is labeled but its outline is not shown on the sketch. Even though the toe segment to the north is inactive, it rests on deposits from the old, inactive part of the Slumgullion landslide (Fig. 4*A* and 4*B*). It is therefore believed to be part of the current episode of movement (Fig. 4). As we pass through this zone, we will stop to examine some of the lobate thrust faults shown in Figure 17.

Pond deposits are recognizable in many places on the active landslide by their uniform tan color and silty texture. About 2.8 km downhill from the active landslide head and about 0.6 km uphill from the front of the active toe, there is an extensive area (80 m by 80 m) of pond deposits (Fig. 7*B* and 17). These deposits begin near line **P-P'**, directly downslope from hummocky, thrust-faulted topography (Fig. 17). The area no longer contains a pond; the surface has been tilted northward to the point that a small stream that formerly fed the pond now flows across the north side of the pond deposits and continues downhill (Fig. 18). A few remnant spruce trees stick partly out of the sediment and small aspen and spruce trees are growing in the sediments near the downhill edge of the former pond (Fig. 18). The downhill edge is at a broad break in slope that separates surfaces that are tilted uphill and downhill. The position of the break in slope has apparently remained fixed about 100 m downhill from the thrust faults.

The pond sediments extend downslope at least 250 m beyond the edge of the pond (Van Horn, written communication, 1994). We will walk through hummocky, deformed pond deposits later as we cross Zone 6. Apparently, the location of the pond has remained fixed while the landslide material has been displaced across the pond site. Fixed features have also been observed at other landslides (Fleming and others, 1988; Baum and others, 1993). Given the current rate of movement at the pond site, the position of the pond apparently has remained fixed for about 100 years and perhaps longer (Van Horn, written communication, 1994).

Parise and Guzzi (1992) suggested that the pond sediments and thrust faults mark the initial position of the toe of the reactivated Slumgullion landslide. Observations at the tip of the currently active toe indicate that it is moving along the surface of the old landslide deposits in bulldozer fashion toppling and overriding trees as it goes. Upslope of the area of thrust faults (uphill of **N-N'**), the reactivated landslide appears to be formed within the older deposits and not sliding on top of them. Parise and Guzzi (1992) noted that if the rate of movement of the toe of the reactivated landslide has remained constant at a maximum of about 2 m/year, the toe should have moved from the upper end of the pond deposits to **R-R'** in about 300 years. Three hundred years is the approximate age that Crandell and Varnes (1961) suggested for the reactivation.

The process of formation and preservation of the pond is outlined in Figure 19, which is a sketch showing the influence of the shape of the failure surface on the morphology of the landslide. The response to the collapse of the north side of the scarp and loading in the head of the inactive landslide apparently triggered the reactivation. Fractures propagated rapidly downslope through the inactive landslide material to the approximate position of the pond. There, the fracture along the basal failure surface emerged to the ground surface (Fig. 19*B*). From this point on, the reactivated landslide advanced over the surface of the old, inactive landslide. While the explanation for the positions of the thrust faults and the pond deposits is consistent with observations, the mechanism has not been documented.

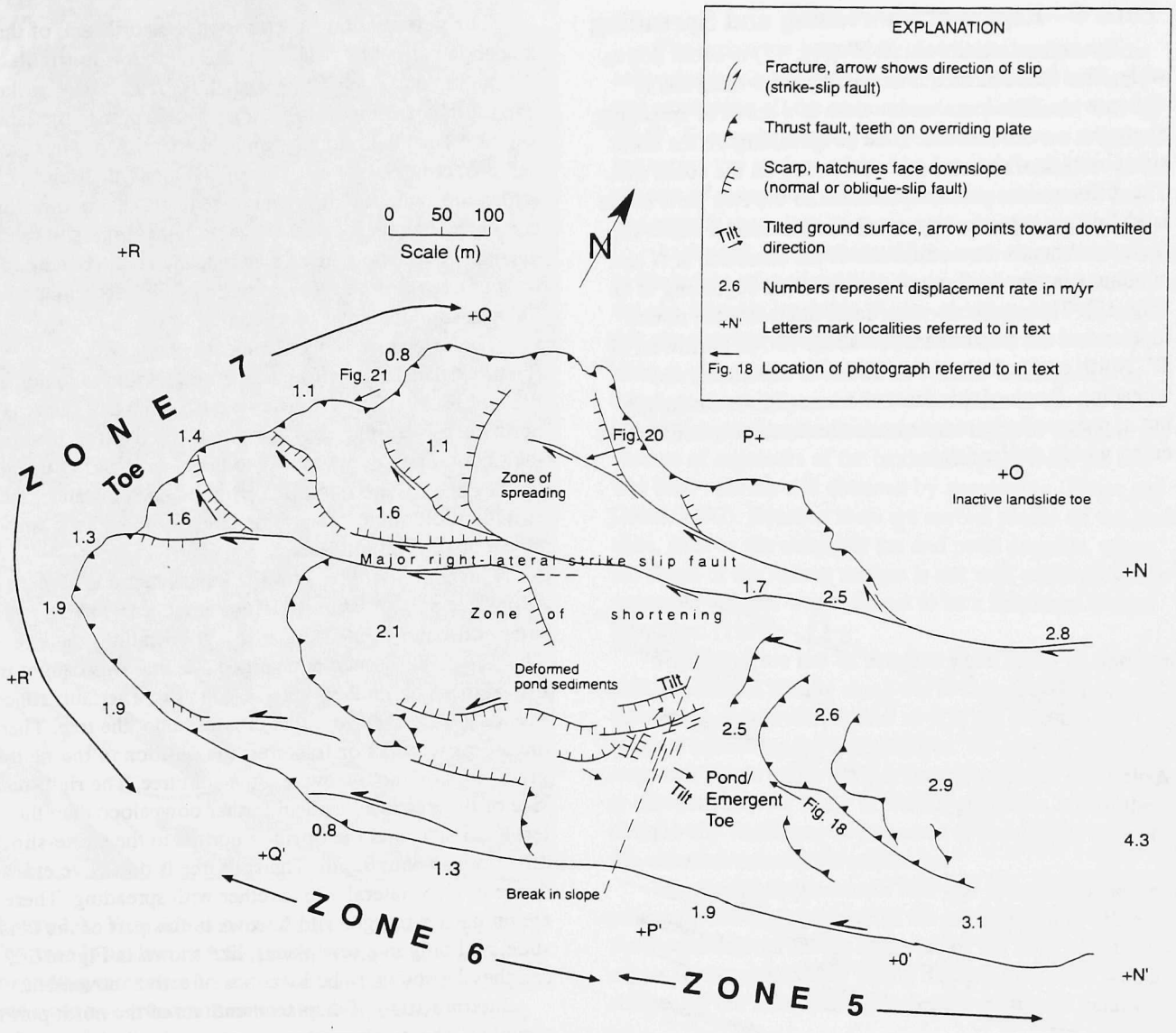

Figure 17. Simplified map of lower part of the active landslide, Zones 5, 6, and 7. Features shown include thrust faults and tension cracks of Zone 5, Pond Deposits and Emergent Toe, and the thrust and oblique-slip faults of Zone 6, Shortening and Spreading, and Zone 7, Active Toe.

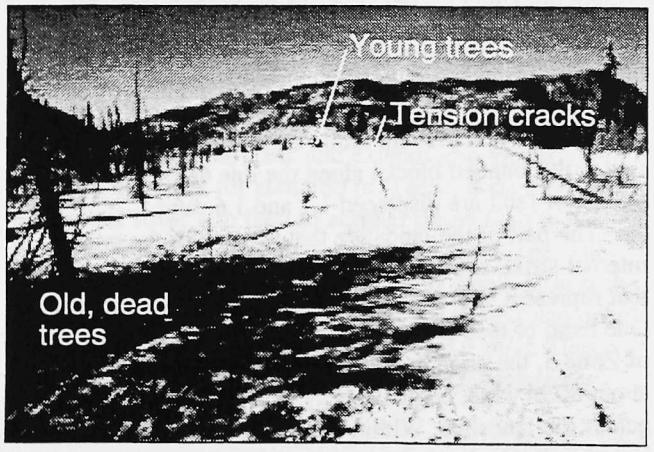

Figure 18. Pond sediments of Zone 5, viewed from inlet, looking west-southwest.

Zone 6—Region of Shortening and Spreading

The active landslide at **N-N'** (Fig. 17) is about 260 m wide. Five hundred meters downslope, the landslide is 430 m wide. This increase in width is a result of spreading along the north flank. The zone of spreading on the north side contrasts with a zone of shortening on the south side. The different kinematic expressions of the two parts of the landslide are separated by a major, right-lateral strike-slip fault that bounds the north flank of the landslide at **N** and continues internally through the landslide beginning at **O** (Fig. 17). This major dividing fault intersects the downslope end of the active landslide about 150 m northwest of **R'**. North of this fault, the landslide is advancing and spreading. South of this fault, the landslide is advancing but at progressively reduced rates because of internal shortening within the landslide.

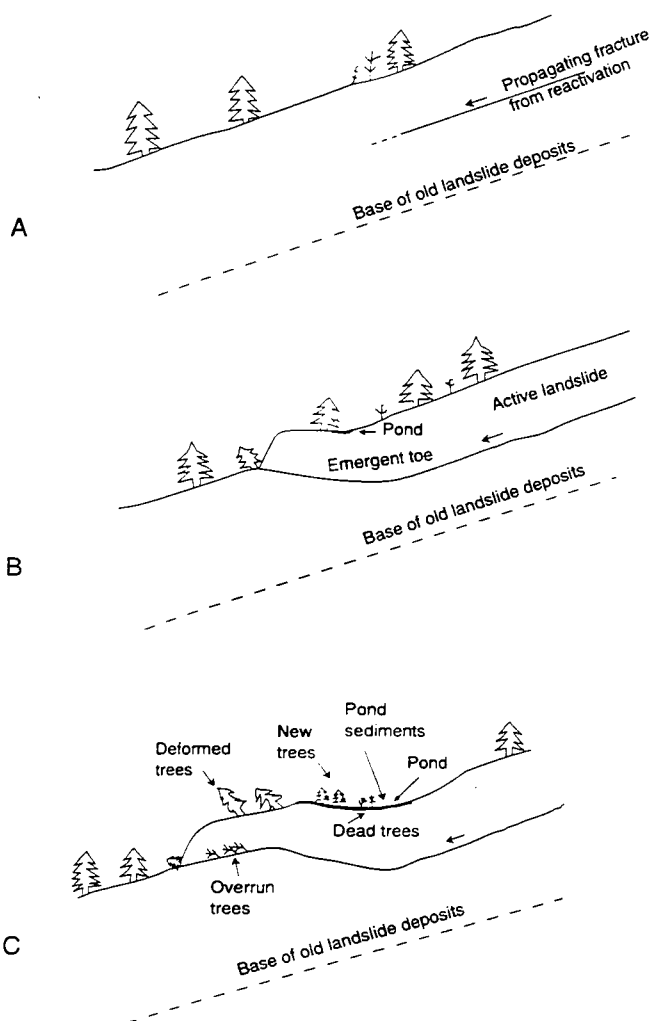

Figure 19. Sketch of concept of pond formation in conjunction with emergent toe of reactivated movement.

The deformation structures on the north side of the landslide consist of strike-slip and oblique-slip (right-lateral slip and opening or spreading) faults. Pure strike-slip faults are difficult to identify in this part of the landslide because the crumbly landslide debris does not preserve fractures well. In a few places along the trend of a strike-slip fault, a scarp is produced, and the fault position can be accurately located. Where a pure strike-slip fault changes orientation, a scarp is produced and stretched roots or split trees (Fig. 20) reveal that the fault accommodates oblique slip indicative of spreading of the toe.

The spreading is accommodated by these oblique-slip fractures. The major strike-slip fault bounding the north flank at **N** divides at **O** into two parts. One part curves northwesterly (obliquely) down to the active toe. The main fault continues southwesterly to between **P** and **Q** where it divides again, here into three parts. In each instance, the curving fault trends toward the landslide boundary and apparently accommodates oblique slip.

The entire north side of the landslide toe is composed of oblique-slip structures. Deformation across these structures consist of right-lateral slip and opening/spreading. This is well illustrated at a spruce tree that was caught in one of these oblique-slip zones (Fig. 20). The fault zone occupies a small furrow that crosses under the tree. There are no open cracks or fractures; the position of the fault is given only by the furrow and the split tree. The right-hand side of the tree is about 1 m farther downslope than the left-hand side, and the opening normal to the strike-slip direction is about 0.8 m. The split tree is definitive evidence of right-lateral slip together with spreading. There are numerous troughs and furrows in this part of the landslide, and only in a few places, like shown in Figure 20, can they be shown to be locations of active movement.

Interpretation of displacement rate of the north part is complex. The displacement progressively diminishes along the major, strike-slip dividing fault from 2.8 m/yr near **N** to 2.5 m/yr just downhill from the first division of the fault. Annual displacement rate decreases to 1.7 m/yr about 50 m further downhill. This change in displacement rate, however, reflects movement of the south side of the major strike-slip fault relative to the north side. Movement rate of material on the north side of the fault near **P** relative to the boundary is unknown. Farther downhill, where the major fault divides into three parts, more displacement is transferred to the oblique-slip faults on the north side such that two fault-bounded blocks along the line **Q-Q'** and north of the major fault are displaced 1.1 and 1.6 m/yr.

The part of the landslide that is south of the major internal strike-slip fault contains two bands of internal toes that represent shortening of landslide material (Fig. 17). One band of toes is the thrust fault described above as part of Zone 5, the pond sediments and emergent toe. The band, about 80 m wide, begins near **N'** and extends obliquely across the landslide. Within the band, the thrust faults consist of individual, overlapping fault segments. Based on the

Figure 20. View of split tree in Zone 6, looking uphill. The tree is broken in four parts by right-lateral and spreading movement. Fault that causes rupture of the tree does not create a fracture at the ground surface, but does form a linear trough about 1 m deep.

change in annual displacement (Fig. 17), there is more than 1 m/yr of shortening across this internal toe.

The next band of thrust faults begins along the south flank about 80 m downhill from **P'**. The thrusting is confined to a much narrower band and many of the shortening features within the band might be inactive. The band consists of a northwest-trending thrust fault that apparently connects to the south flank and extends continuously into the landslide body for about 60 m. There, it steps along a left-lateral strike-slip fault to another thrust fault that extends to the major internal, strike-slip fault zone. The amount of shortening across this band is small. Rate at the downslope toe of the landslide **R-R'** is 1.9 m/yr and uphill from the internal toe (between **Q-Q'**) is 2.1 m/yr. Thus, annual shortening across this internal toe is apparently about 0.2 m/yr.

Zone 7—Active Toe

The active toe bounds the downhill terminus of the active landslide beginning about 25 m from **O** toward **P** and continuing all the way around the perimeter, **O-P-Q-R'-Q'**. Everywhere along the perimeter, the toe is advancing across the surface of the old, inactive landslide. In the process of overriding the landscape, it pushes trees over and engulfs them into the base of the landslide (Fig. 21).

At the toe, the thickness of the active landslide is equal to the height of the landslide above the projected surface of the old, inactive landslide. Parise and Guzzi (1992) used this observation to estimate the volume of the active landslide at about 20 x 10^6 m^3. The volume estimation was based on the thickness of active landslide at the toe combined with displacement vectors and slope to compute the volume of segments of the landslide uphill from the toe. The total volume was obtained by summation (Parise and Guzzi, 1992). Because there are several places on the landslide, such as the emergent toe and pond deposits, where the shape of the failure surface is not well understood, the estimated volume was believed to be a minimum (Parise and Guzzi (1992).

The active toe has an irregular trace along its northern half. Superficial sliding along the oversteepened front of the toe has obscured fractures so it is not possible to observe causes for the irregularities. We assume that the steps and bends along the terminus are a result of a velocity discontinuity. At many of the irregularities, one of the oblique-slip faults can be projected to the general area of the assumed velocity discontinuity.

The annual displacement rate was measured at seven points around the perimeter of the toe between **Q-Q'**. All the measurements except the value of 1.3 m/yr near the terminus were measured by taping distances between wooden stakes. All the measured distances are minimum values

Figure 21. View of north side of active toe (Zone 7) where trees are being overridden by bulldozer-like movement of the landslide. Moving ground on left pushes trees over and buries them.

because of possible differences between measurement and movement directions. The value of 1.3 m/yr mentioned above is also a minimum because measurement points extended only about 10 m onto actively moving material.

In the place on the active toe where we were measuring displacement rate by surveying rather than simply taping distances, we were able to determine the displacement vector of the active toe relative to nonmoving ground farther downhill. We expected that the displacement would be approximately parallel to the slope because it is obviously advancing over old landslide debris. To our surprise, we found that the displacement is directed nearly horizontally out of the slope. This condition, which tends to thicken the toe, apparently is the result of accumulation of trees and other debris along the contact between moving and nonmoving ground (Fig. 21). Displacement tends to steepen the front of the active toe. Sloughing of materials on the oversteepened face gives rise to a churning of material along the active front and the advance is similar to the motion of the tread of a bulldozer. Continuing movement results in continuing thickening of the toe.

Deformed Area Ahead of Active Toe

In 1991, Varnes and others (1996) began to investigate possible movements on the inactive part of the landslide below the active toe to determine the effects of loading by the active toe. Initially, they laid out loops of level circuits (we will see some of the points on the circuits on the way back to the bus). During the first year, points close to the active toe subsided as much as 20 mm and points 50-100 m away from the toe subsided smaller but observable amounts. Subsequently, a triangulation-trilateration net was added to observe possible horizontal movements. Continued observations have confirmed that ground is depressed in front of the active toe except at three points where the ground rose 20-80 mm in 2 years. Two of these points were on prominent rolls at the northwest edge of the toe. Small horizontal movements have also been detected but no clear pattern of horizontal movements has emerged from the data.

REFERENCES

Atwood, W. W., and Mather, K. F., 1932, Physiography and Quaternary geology of the San Juan Mountains, Colorado: U.S. Geological Survey Professional Paper 166, 176 p.

Burbank, W.S., 1947, Lake City area, Hinsdale County, *in* Mineral Resources of Colorado: Colorado Mineral Resources Board, p. 439-443.

Baum, R. L., and Fleming, R. W., 1996, Kinematic studies of the Slumgullion landslide, Hinsdale County, Colorado, Chapter 2 *in* Varnes, D. J. and Savage, W. Z., eds., The Slumgullion Earth Flow: A Large Scale Natural Laboratory: U.S. Geological Survey Bulletin 2130, p. 9-12.

Baum, R. L., and Fleming, R. W., 1991, Use of longitudinal strain in identifying driving and resisting elements of landslides: Geological Society of America Bulletin, v. 103, p. 1121-1132.

Baum, R. L., Fleming, R. W., and Johnson, A. M., 1993, Kinematics of the Aspen Grove landslide, Ephraim Canyon, central Utah, chap. F *of* Landslide processes in Utah—Observation and theory: U.S. Geological Survey Bulletin 1842, p. F1-F34.

Chleborad, A.F., 1996, Radiocarbon age of a newly identified Slumgullion landslide deposit, Chapter 5 *in* Varnes, D. J. and Savage, W. Z., eds., The Slumgullion Earth Flow: A Large Scale Natural Laboratory: U.S. Geological Survey Bulletin 2130, p. 29-34.

Chleborad, A. F., 1993, Description, origin, and implications of a newly identified Slumgullion landslide deposit, San Juan Mountains, Southwestern Colorado: U.S. Geological Survey Open-File Report 93-548, 16 p.

Chleborad, A.F., Diehl, S.F., and Cannon, S.H., 1996, Geotechnical properties of selected materials from the Slumgullion landslide, Chapter 11 *in* Varnes, D. J. and Savage, W. Z., eds., The Slumgullion Earth Flow: A Large Scale Natural Laboratory: U.S. Geological Survey Bulletin 2130, p. 67-71.

Crandell, D.R., and Varnes, D.J., 1960, Slumgullion earthflow and earthslide near Lake City, Colorado [abs.]: Geological Society of America Bulletin, v. 71, no. 12 pt. 2, p. 1846.

_____1961, Movement of the Slumgullion earthflow near Lake City, Colorado, *in* Short Papers in the Geologic and Hydrologic Sciences: U.S. Geological Survey Professional Paper 424-B, p. B136-B139.

Diehl, S.F., and Schuster, R.L., 1996, Preliminary geologic map and alteration mineralogy of the main scarp of the Slumgullion landslide, Chapter 3 *in* Varnes, D. J. and Savage, W. Z., eds., The Slumgullion Earth Flow: A Large Scale Natural Laboratory: U.S. Geological Survey Bulletin 2130 p. 13-19.

Endlich, F. M., 1876, Report of F. M. Endlich, *in* U.S. Geological and Geographical Survey (Hayden) of the Territories Annual Report 1974, p. 203.

Fleming, R. W., Baum. R. L., and Johnson, A. M., 1993, Deformation of landslide surfaces as indicators of movement processes, *in* Proceedings of the 2nd Seminar on Landslide Hazards, Cosenza, Italy, March 5-6, 1990: Geographica Fisica e Dinamica Quaternaria, v. 16, no. 1, p. 9-11.

Fleming, R. W., and Johnson, A.M., 1989, Structures associated with strike-slip faults that bound landslide elements: Engineering Geology, v. 27, p. 39-114.

Fleming, R. W., Johnson, R. B., and Schuster, R. L., 1988, The reactivation of the Manti landslide, Chap. A *of* The Manti landslide, Utah: U.S. Geological Survey Professional Paper 1311, p. 1-22, 1 Pl.

Gomberg, J.S., Bodin, P.W., Savage, W. Z., and Jackson, M. E., 1995, Landslide faults and tectonic faults, analogs?: The Slumgullion earthflow, Colorado: Geology, v. 23, no. 1, p. 41-44.

Guzzi, R., and Parise, M., 1992, Surface features and kinematics of the Slumgullion landslide near Lake City, Colorado: U.S. Geological Survey Open-File Report 92-252, 45 p.

Howe, E., 1909, Landslides in the San Juan Mountains, Colorado: U.S. Geological Survey Professional Paper 67, 45 p.

Keefer, D.K., and Johnson, A.M., 1983, Earth flows: morphology, mobilization, and movement: U.S. Geological Survey Professional Paper 1264, 56 p.

Larsen, E.E., 1913, Alunite in the San Cristobal quadrangle, Colorado: U.S. Geological Survey Bulletin 530-F, p. 179-183.

Lipman, P. W., 1976, Geologic map of the Lake City caldera area, western San Juan Mountains, southwestern Colorado: U.S. Geological Survey Miscellaneous Investigations Series Map I-962, scale 1:48,000.

Madole, R.F., 1996, Preliminary chronology of the Slumgullion landslide, Hinsdale County, Colorado, Chapter 1 *in* Varnes, D. J. and Savage, W. Z., eds., The Slumgullion Earth Flow: A Large Scale Natural Laboratory: U.S. Geological Survey Bulletin 2130, p. 5-7.

Parise, M., and Guzzi, R., 1992, Volume and shape of the active and inactive parts of the Slumgullion landslide, Hinsdale County, Colorado: U.S. Geological Survey Open-File report 92-216, 29 p.

Savage, W. Z., and Fleming, R. W., 1996, Slumgullion landslide fault creep studies, Chapter 12 *in* Varnes, D. J. and Savage, W. Z., eds., The Slumgullion Earth Flow: A Large Scale Natural Laboratory: U.S. Geological Survey Bulletin 2130, p. 73-76.

Schuster, R.L., 1996, Slumgullion landslide dam and its effects on the Lake Fork, Chapter 6 *in* Varnes, D. J. and Savage, W. Z., eds., The Slumgullion Earth Flow: A Large Scale Natural Laboratory: U.S. Geological Survey Bulletin 2130, p. 35-41.

Smith, W. K., 1993, Photogrammetric determination of movement on the Slumgullion slide, Hinsdale County, Colorado, 1985-1990: U.S. Geological Survey Open-File Report 93-597, 17 p., 2 Pl.

Varnes, D. J., and Savage, W. Z., eds., 1996, The Slumgullion Earth Flow: A Large Scale Natural Laboratory: U.S. Geological Survey Bulletin 2130, 95 p.

Varnes, D.J., Smith, W.K., Savage, W.Z., and Powers, P.S., 1996, Deformation and control surveys, Slumgullion landslide, Chapter 7 *in* Varnes, D. J. and Savage, W. Z., eds., The Slumgullion Earth Flow: A Large Scale Natural Laboratory: U.S. Geological Survey Bulletin 2130, p. 43-49.

Williams, R.A., and Pratt, T.L., 1996, Detection of the base of Slumgullion landslide, Colorado, by seismic reflection and refraction methods, Chapter 13 *in* Varnes, D. J. and Savage, W. Z., eds., The Slumgullion Earth Flow: A Large Scale Natural Laboratory: U.S. Geological Survey Bulletin 2130, p. 77-83.